Final Report

INVESTIGATION OF PKP SEISMIC WAVES

STANFORD RESEARCH INSTITUTE
SRI-Irvine · Irvine, California 92664 · U.S.A.

STANFORD RESEARCH INSTITUTE
Menlo Park, California

Final Report *September 1970*

INVESTIGATION OF PKP SEISMIC WAVES

By: WILLIAM F. ISHERWOOD

Prepared for:

DIRECTOR OF PHYSICAL SCIENCES
AIR FORCE OFFICE OF SCIENTIFIC RESEARCH
WASHINGTON, D.C. 20333
Attention: SRPG

ARPA Order: 292, Amend. No. 43
Project Code: 7F10
Name of Contractor: Stanford Research Institute
Date of Contract: 1 February 1967
Amount of Contract: $131,188
Contract Number: F44620-67-C-0080
Project Scientist: William F. Isherwood
Title of Work: Investigation of PKP Seismic Waves
SRI Project PHU-6495

Approved:

D. R. GRINE, *Manager*
Geophysics Program

GEORGE R. ABRAHAMSON, *Director*
Poulter Laboratory
Physical Sciences Division

CHARLES J. COOK, *Executive Director*
Physical Sciences Division

CONTENTS

FIGURES

TABLE

FOREWORD

This final report is a documentation of the work done under contract F44620-67-C-0080, Investigation of PKP Seismic Waves. Details of the project history, data gathering operations, and results of preliminary examination of the data were presented in an Annual Report issued March 15, 1969, and are only summarized in this report. Project results and conclusions are presented here.

Stanford Research Institute's participants in the project were as follows: C. W. Smith, Physicist; W. F. Isherwood, Geophysicist; D. E. Wolf, Mathematician; and J. D. Eisler, Senior Geophysicist. Initial project supervisor was W. H. Westphal; interim supervisor was R. A. Schmidt, and supervisor for the conclusion of the project is D.R. Grine, Manager, Geophysics Program. Major D. D. Young, AFOSR, acted as initial Project Monitor and also assisted with the installation of the seismic array at Byrd Station.

Bruce A. Bolt, Professor of Geophysics, University of California, Berkeley, acted in a consulting capacity.

INTRODUCTION

Stanford Research Institute (SRI), with support from the Advanced Research Projects Agency (ARPA and the National Science Foundation (NSF), installed a four-element seismic array (BYA) at Byrd Station, Antarctica, beginning operation January 18, 1968. Short period vertical component seismometers were selected in anticipation of high magnification operation. Figures 1 and 2 show the plan of the BYA array and a block diagram of the system. The March 15, 1969, Annual Report (Isherwood, 1969) describes in detail the system and the data gathering operations. The site was selected to study core phase arrivals because PKP waves have a principal focus at an angular distance, Δ, of approximately 142° from the source, and Byrd Station is close to 142° from several of the great seismic zones in the Northern Hemisphere, as shown in Figure 3.

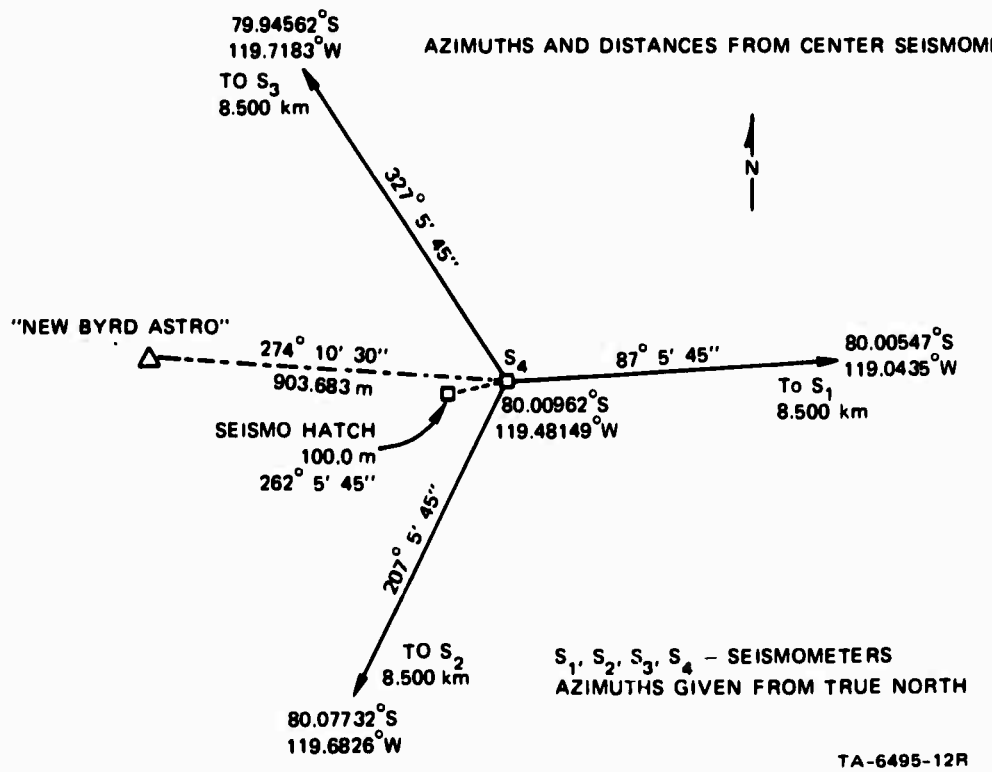

FIGURE 1 PLAN OF BYA SEISMIC ARRAY

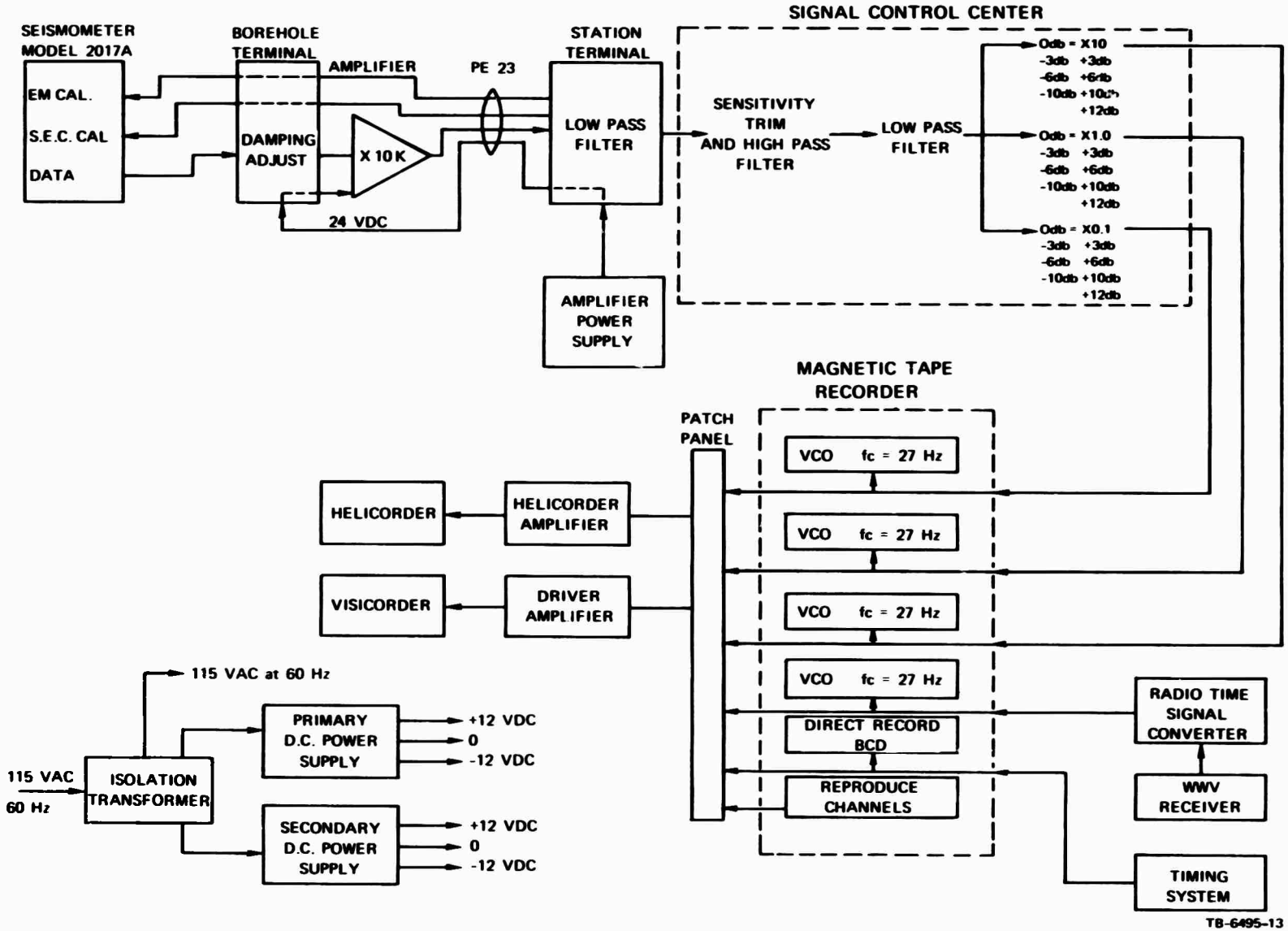

FIGURE 2 BLOCK DIAGRAM—TYPICAL CHANNEL

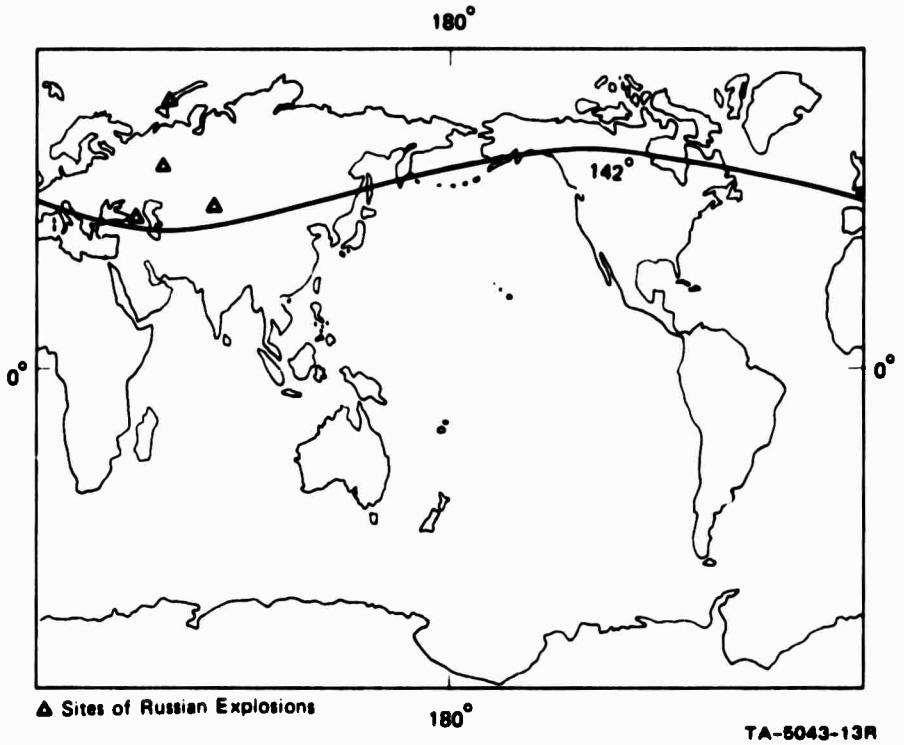

FIGURE 3 142° GEOCENTRIC DISTANCE FROM BYRD

Helicorder and magnetic tape records for the period January 18, 1968, through November 24, 1969, including approximately 1000 core phase arrivals, were analyzed. The objectives of the research contracted between ARPA and SRI were as follows:

1. To establish and prepare specifications for a high-quality seismograph station capable of recording PKP seismic waves to operate in Antarctica during the year of 1968.

2. To study the characteristics of the ambient seismic noise and relate them to oceanic and continental storms.

3. To apply appropriate data processing techniques aimed at enhancement and identification of PKP waves in the presence of ambient seismic signals and noise.

4. To analyze and interpret PKP wave data in terms of their source characteristics and the internal constitution of the earth.

Since the above interpretations depend on accurate travel time prediction, BYA-observed travel times were compared with published tables as an inseparable objective.

Initial evaluation was based on the origin times, hypocenters, and magnitudes published by the U. S. Coast and Geodetic Survey (USC&GS). Events listed herein are referred to by the USC&GS origin times.

Nomenclature will follow that of Jeffreys and Bullen (1967) and Bolt (1968). Figure 4 presents the PKP travel time curve for reference throughout the text.

RESULTS

Seismic Noise

Although background noise level varied with time, Byrd Station was found to be a fairly quiet seismic site, especially within the band of PKP frequencies. Helicorder records were generally made with a system magnification near 100 K. Typically, higher noise levels were observed for periods of one to two weeks interspersed with longer periods of low noise levels.

The seismometers were buried at a depth of $\sim$ 60 m, providing adequate insulation from direct vibration by local winds. Inspection of the records showed no correlation between the seismic noise level and local storms; many severe local storm occurred during periods of low noise. The months of March and April 1968 present an example: During March, the records were generally noisy with the most noise from about the 10th to 19th. Wind records for this period show a two-day storm on the 13th and 14th but show lower average winds and peak gusts than later in the month. April, which set a record monthly average wind speed of 27.1 mph, had relatively low noise levels.

Correlation of noise levels with oceanic storms was prevented by lack of meteorological data for the oceans near the Byrd Land coast. According to the Antarctic Support Activities (OIC, Detachment Charlie, personal communication), there were a maximum of five ships in the entire area off the coast in the calendar year 1968, providing almost no meteorological data. State-of-sea determination from satellite pictures

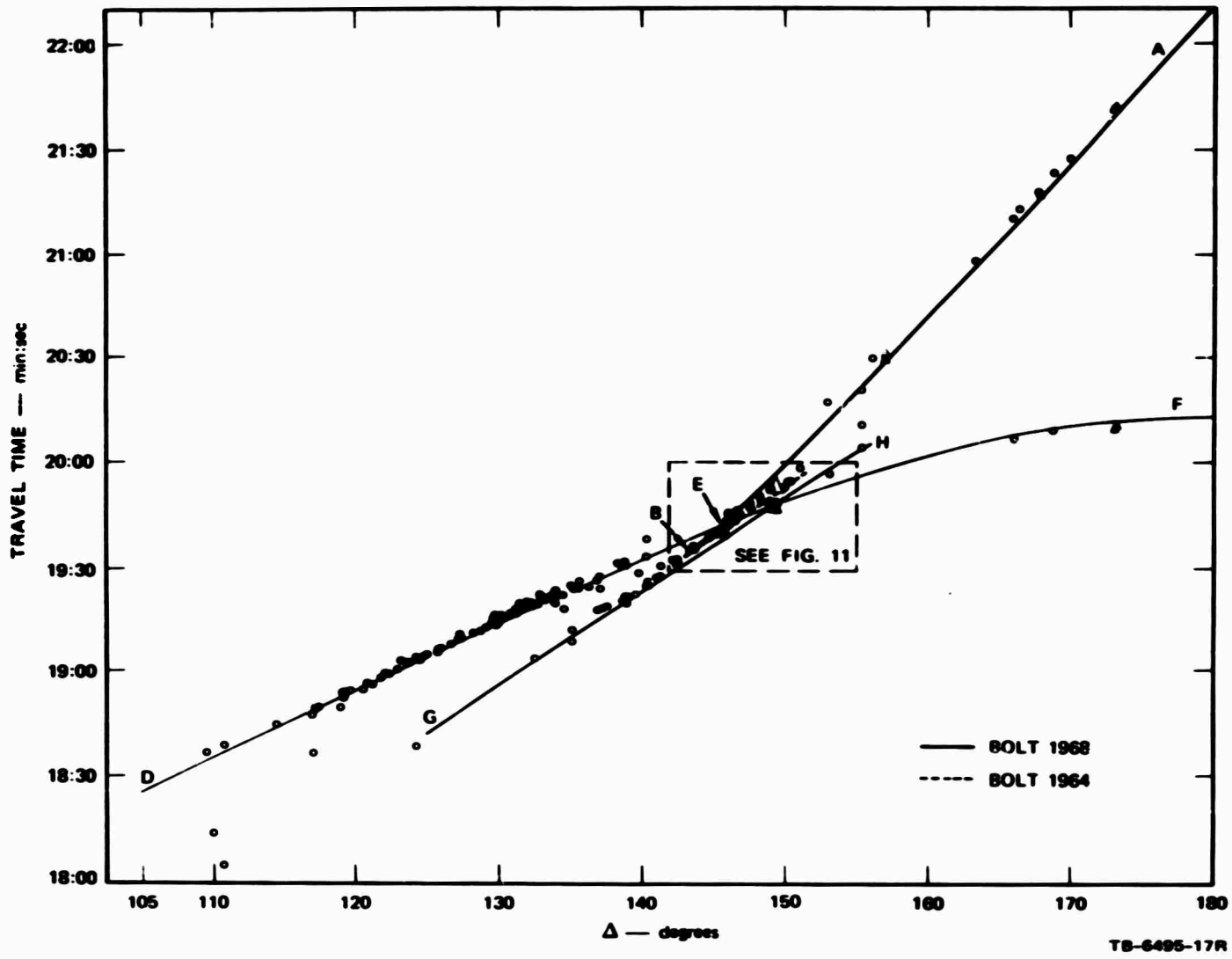

FIGURE 4 BYA TRAVEL TIMES

is, as yet, an unperfected art. Consequently, the surface charts available have a noticeable lack of data for the required ocean area (Figure 5).

Tests were run to determine the frequency content of the ambient noise and the PKP signals. Initial frequency measurements were made by scaling the helicorder records. Later, analog filtering of the magnetic tapes were employed and finally spectral analysis was carried out by digital computer. Figure 6 is a plot showing the frequency spectrum of an average noise sample compared with a typical sample of PKP signal. This clearly shows that the majority of signal energy is contained between 0.4 Hz (2.5 sec period) and 2 Hz (0.5 sec period). The background noise lies mostly at much higher frequencies and slightly lower frequencies than this signal range. Figure 7 shows an extreme case before and after digital filtering with pass band of 0.4 to 2.0 Hz. The large amplitude noise near 5 Hz on Figure 7 is encountered when snow cats are in operation in the station area. Being well out of the signal band, it is the easy target of additional filtering. Natural ground motion presents more of a problem. The greatest natural interference arises from longer period noise, which rises to $\sim$ 30 mμ at 0.3 Hz (as measured from the helicorder) and may be as high as $\sim$ 10 mμ at 0.5 Hz. Signals from 1 to 2 Hz have least competition with background noise, which is generally $<$ 1.5 mμ of ground motion.

Detection Threshold

PKP arrivals were observed at Byrd Station for the range of Δ = 110 to 173^{o}. The amount of energy transmitted, however, varies considerably over this range as pointed out by Shahidi (1968). At distances where more than one arrival are seen, the relative energy from different wave paths also varies with Δ. This is seen both in the amplitudes of arrivals and the quality of the first motion seen. The variation is shown in Figure 8, a composite of PKP arrivals. Table 1 lists the events used in Figure 8. Although an attempt was made to use events of near the same magnitude and use records of near the same gain, the relative amplitudes between different traces means little for such a small sample. Events with Δ's $<$ 140^{o} show early arrivals, corresponding to the GH branch of the travel time curve. These ray-paths transmit so little energy that arrivals are seen only from large events and even then onsets observed were emergent.

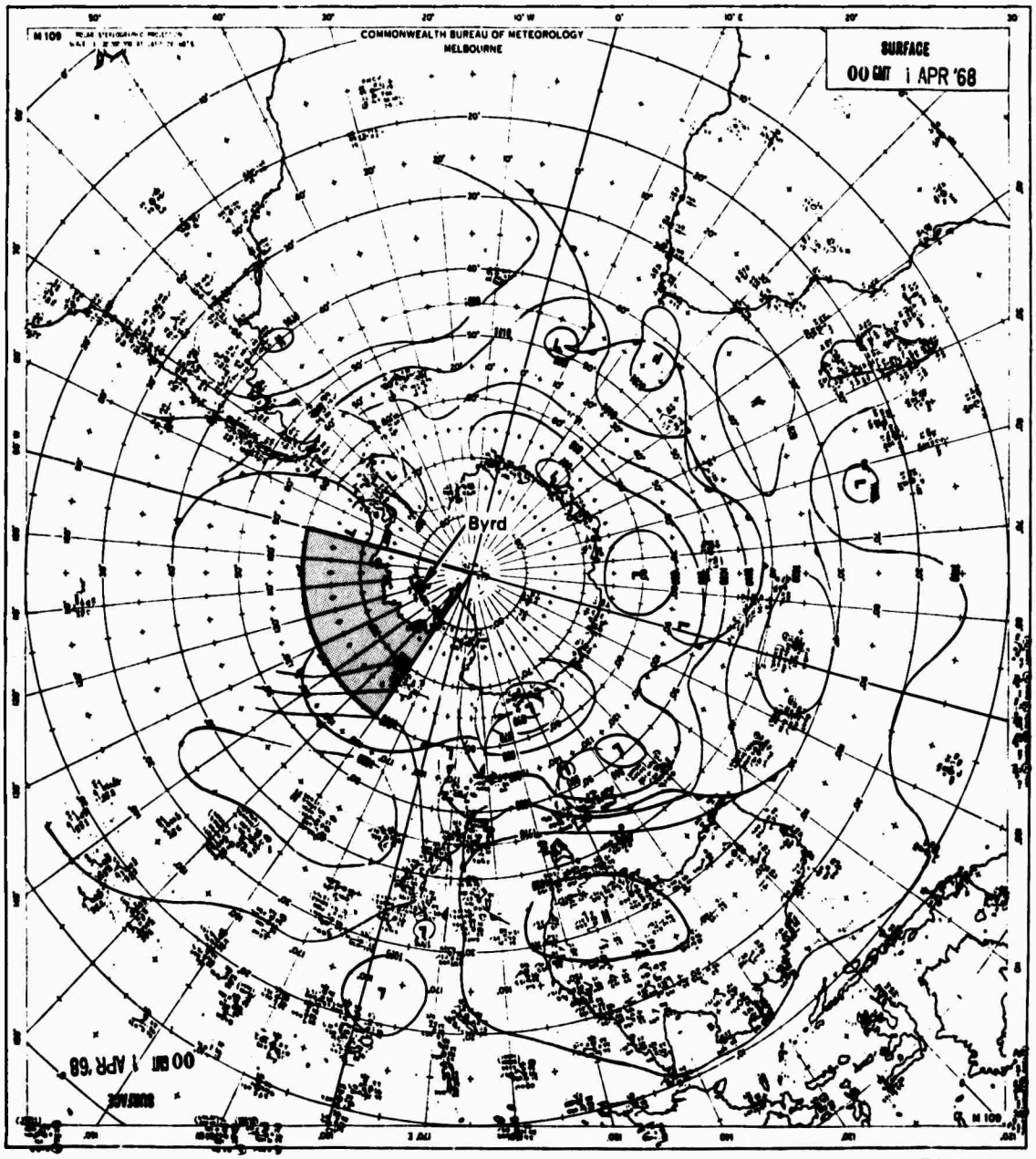

TA-6495-29

FIGURE 5 SURFACE METEOROLOGY

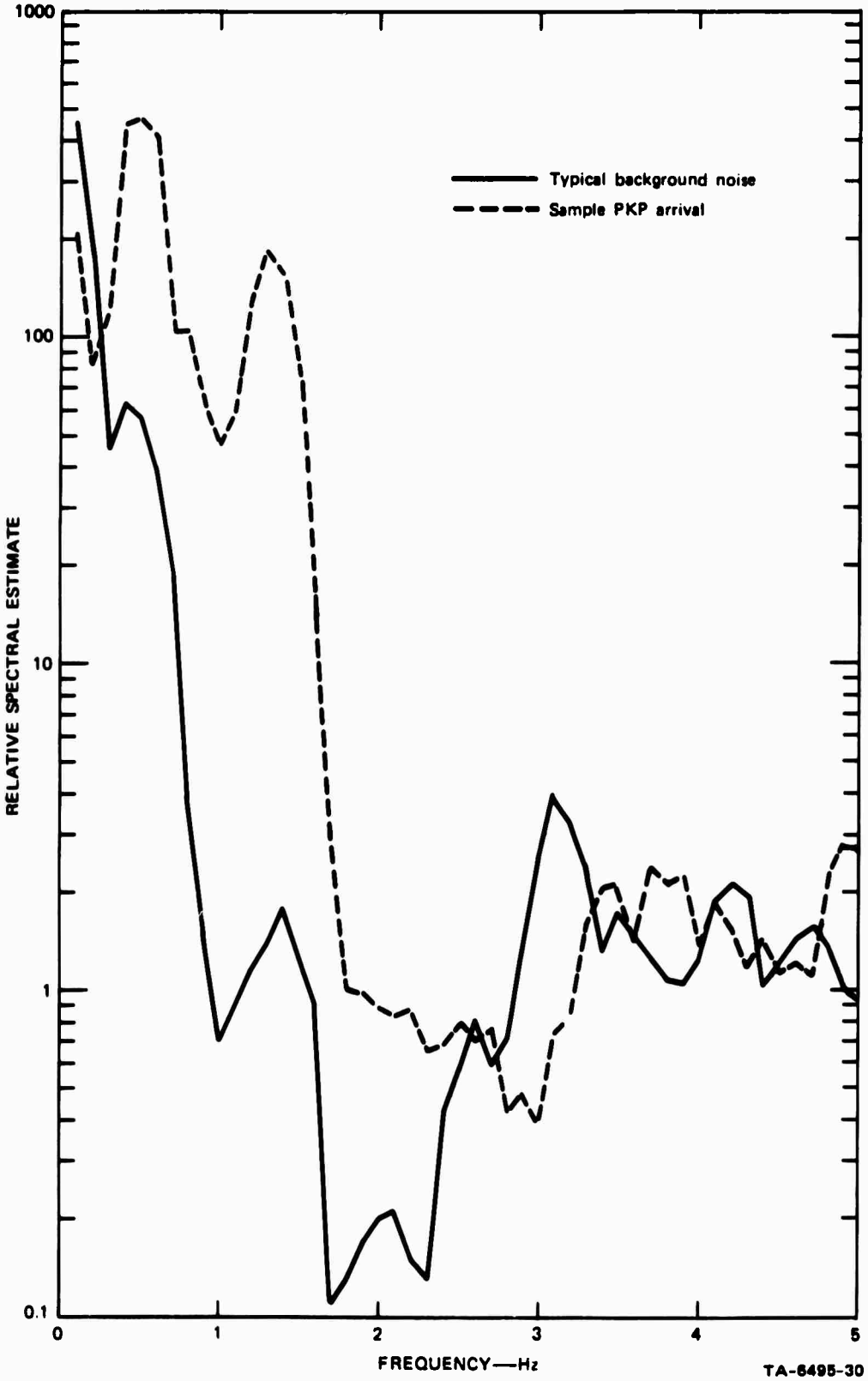

FIGURE 6 SPECTRAL CONTENT OF NOISE AND PKP SIGNAL

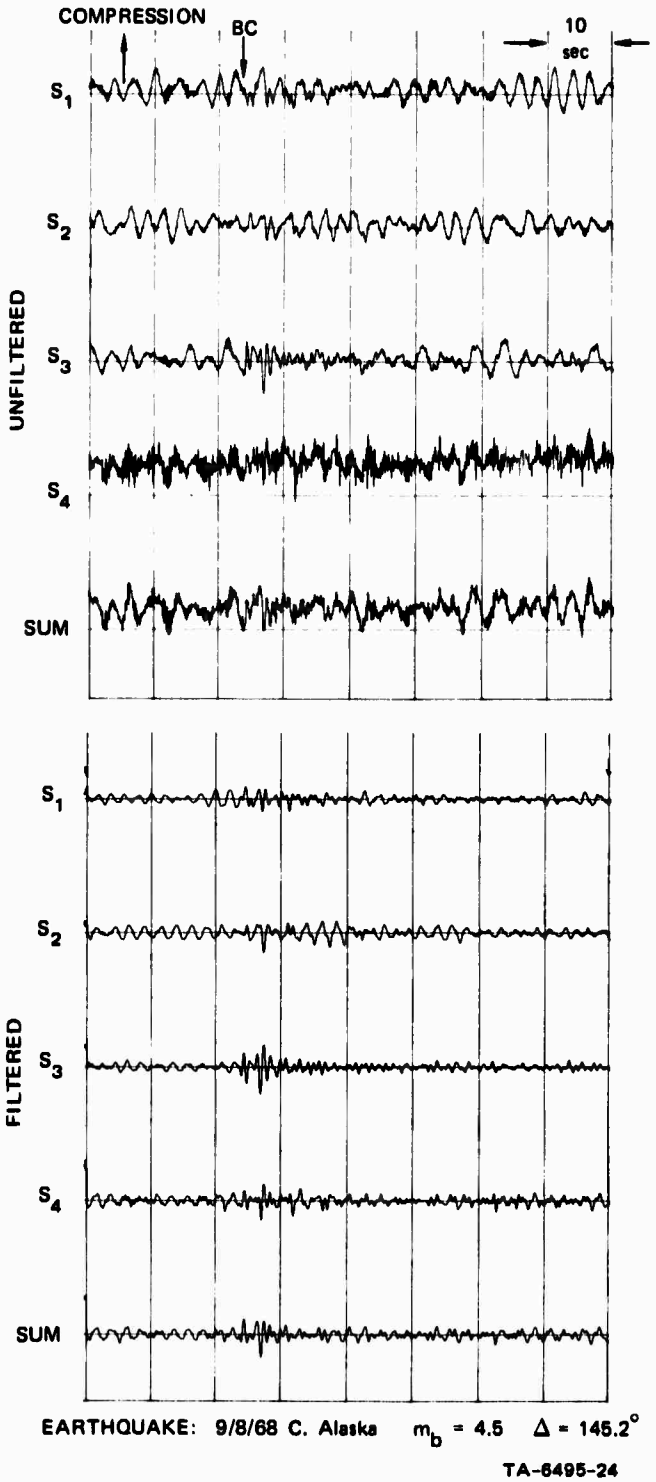

FIGURE 7 EFFECT OF BAND PASS FILTERING (0.4 to 2.0 Hz)

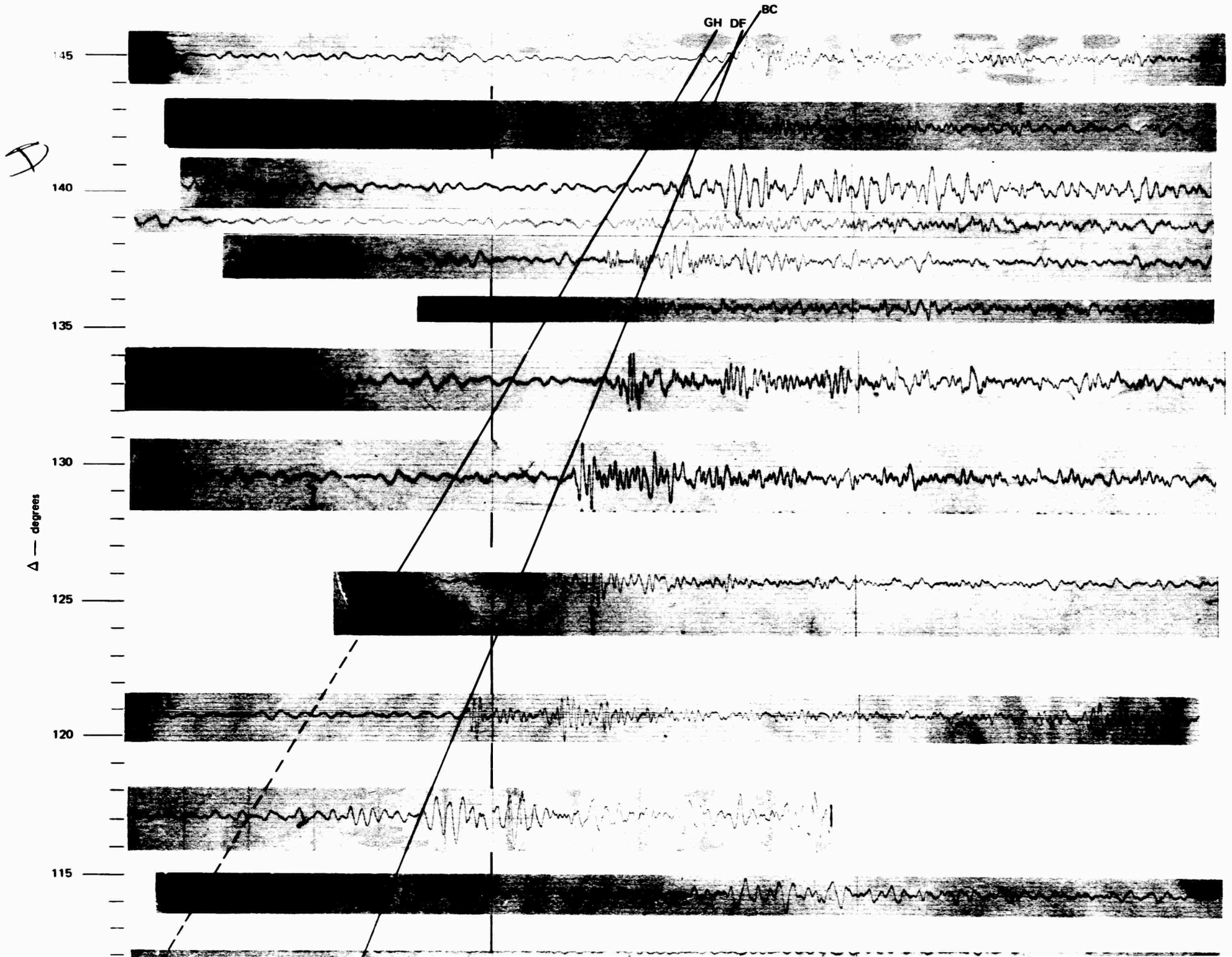
GH
DF
BC
145
140
135
130
125
120
115
Δ — degrees

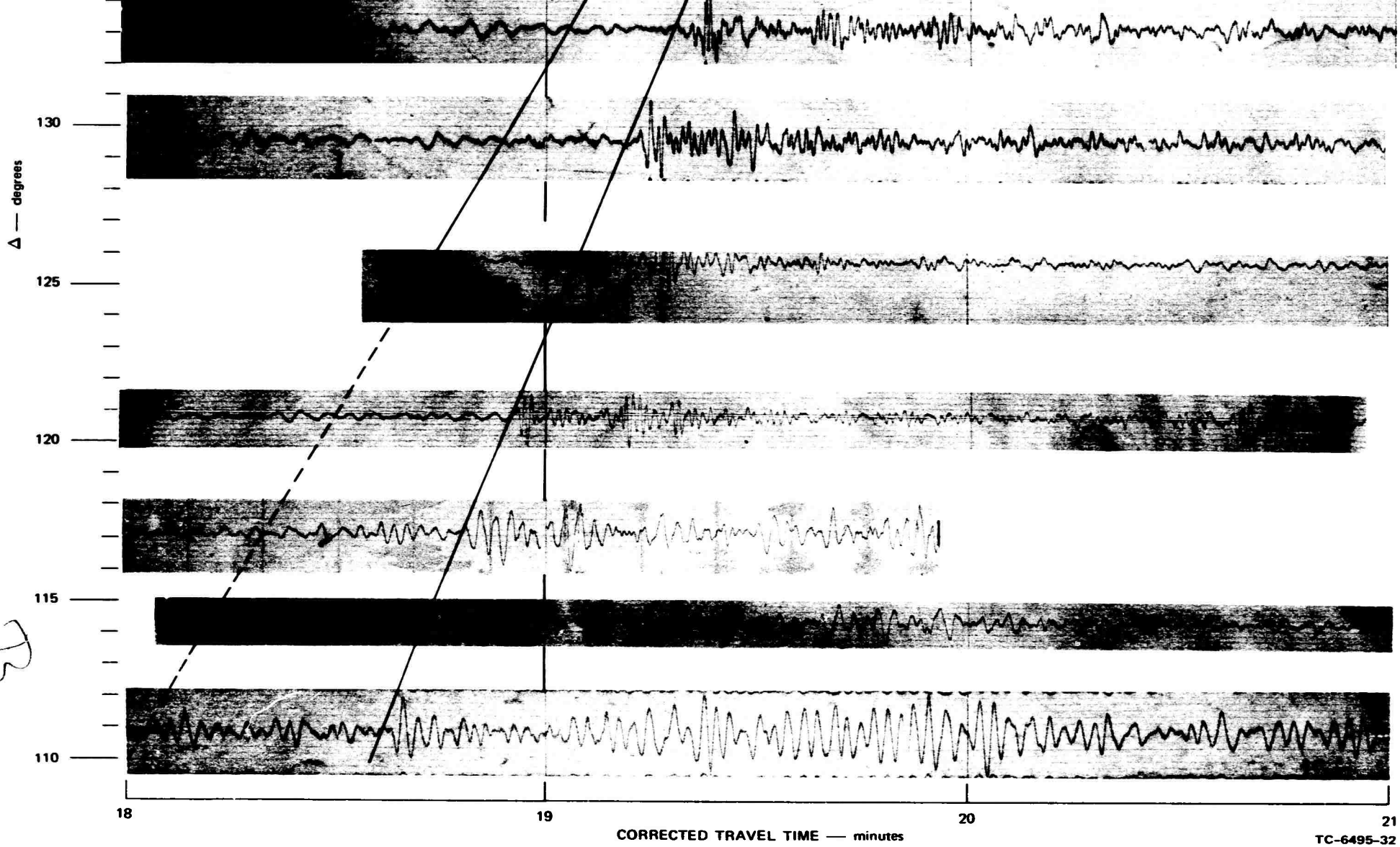

FIGURE 8 PKP COMPOSITE

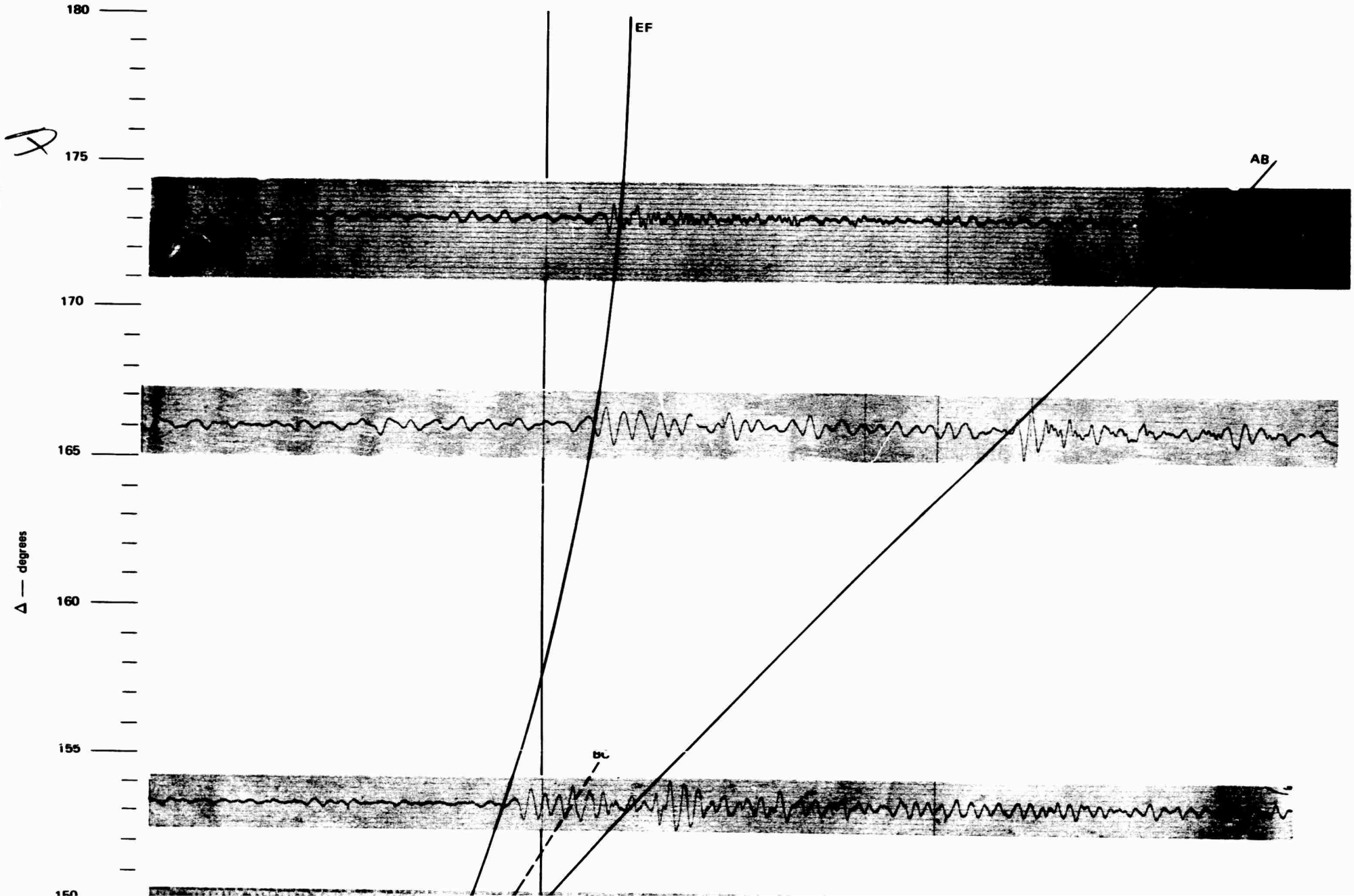
180
175
170
165
160
155
150
Δ — degrees
EF
AB
BC

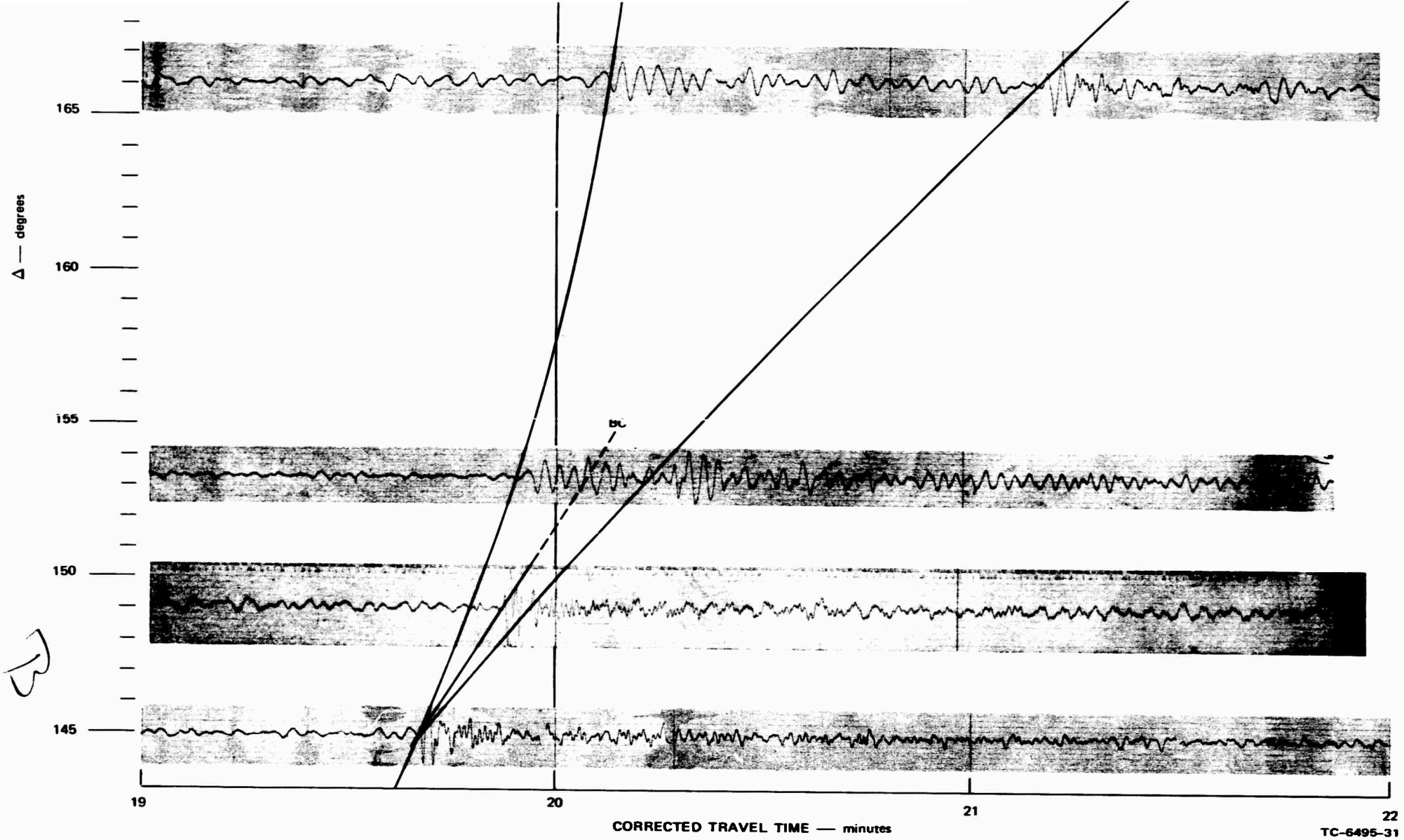

FIGURE 8 PKP COMPOSITE concluded

Table I

EVENTS SHOWN ON FIGURE 8, PKP COMPOSITE

Δ^{o}	Region	Date	m_b	Depth (km)
173.2	Novaya Zemlya	Nov. 7, 1968	6.1	0
166.1	Laptev Sea	Apr. 7, 1969	5.5	33
153.4	Iceland	Dec. 5, 1968	5.5	5
149.1	E. Kazakh	Sep. 5, 1968	5.5	0
145.1	S.W. Russia	Sep.26, 1969	5.6	0
142.3	E. Kamchatka	Jan.22, 1969	5.5	33
140.2	Turkey	Sep. 3, 1968	5.7	5
138.9	Kamchatka	Jun.15, 1968	5.4	39 D
137.5	Kurile Islands	Oct.24, 1968	5.5	35
135.8	Hindu Kush	Dec.19, 1968	5.4	151
133.0	Hokkaido, Japan	Aug. 7, 1968	5.6	54 D
129.7	E. of Honshu, Japan	Jun.12, 1968	5.7	36 D
125.7	Shikoku, Japan	Dec.11, 1968	5.4	32 D
120.7	Ryukyu Islands	Nov.12, 1968	5.8	48 D
117.1	Taiwan	Feb.26, 1968	6.0	24
114.4	Philippines	Nov.10, 1968	5.2	33
110.8	Luzon, Philippines	Aug. 3, 1968	5.9	37

The PKP detection threshold at Byrd Station was determined as a function of Δ by searching the helicorder records for about 500 USC&GS listed events. The curves on Figure 9 show the detection threshold and its variation with Δ from these unfiltered helicorder records. (Not all of the arrivals identified were recognized by the on-site operator.) As would be expected there is some scatter about the lines given. Beyond 150^{o}, the number of events listed by the USC&GS were fewer; consequently, this portion of the figure is poorly determined. Beyond 140^{o}, the arrivals from different branches frequently interfere with each other. A separate curve for EF arrivals is shown where they are distinct. This threshold could no doubt be lowered by providing sharper cutoff analog filters.

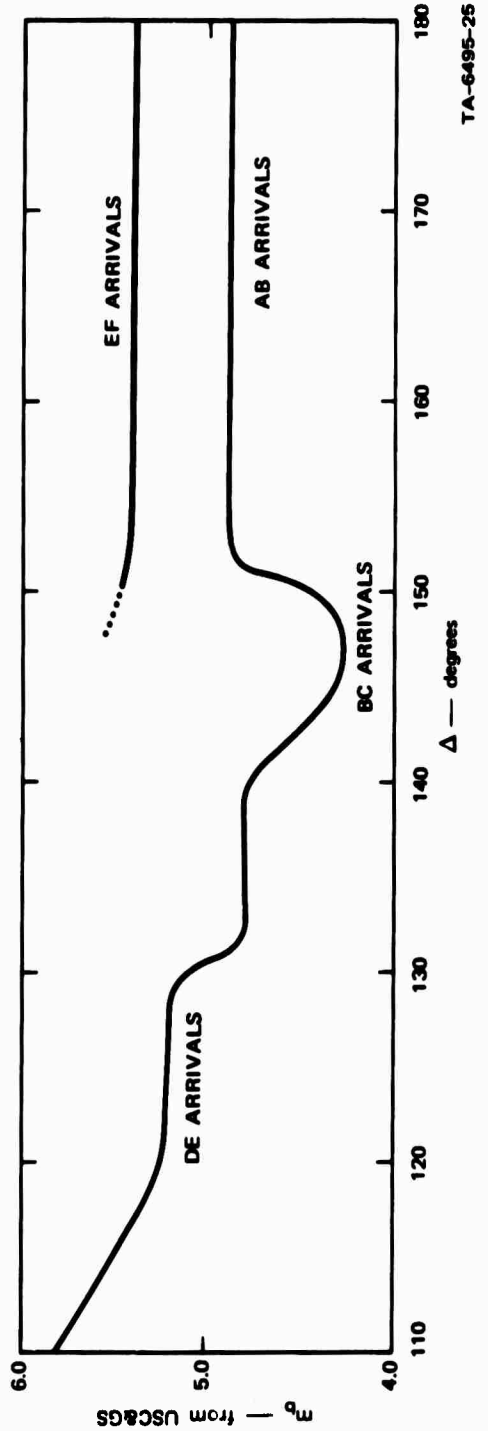

FIGURE 9 DETECTION THRESHOLD

The threshold determined from the helicorder records is not the optimum available from the recorded data. Work is needed to optimize the data and assess the realizeable detection threshold. The magnetic tape data may then be machine processed to lower the threshold.

Data Processing Techniques

Although the present analog system is highly filtered (Figure 10 shows the typical frequency response), the value of further data processing is clearly shown in Figure 7. For computer processing, the records from 142 events were selected and digitized by the Vela Digitizing Center at 50 samples per sec. The first enhancement of PKP arrivals was by digital filtering with a band pass of 0.4 to 2.0 Hz, the results of which were shown previously. These cutoff frequencies were chosen by inspection of the seismograms. No doubt even greater enhancement can be accomplished with optimum filtering--which has not been attempted at this stage.

Summations of the signals from the four seismometers were formed, as well as "lagged sums" as a test of velocity filtering feasibility. Results indicated that a straight sum of the signals was helpful in correlation of significant arrivals, but the BYA array was too small to show additional improvement by velocity filtering. Uncertainty of local geologic influence and relative timing between channels added to the difficulty in interpreting values of apparent velocity observed across the array. (The average of arrival times from the playback of 100 events shows that arrivals on the center seismometer are seen 0.1 sec earlier than on the surrounding three seismometers. Geologic and elevation uncertainties and measured relative phase delays in the electronics cannot account for this difference. At these slow tape speeds, however, relative timing is quite sensitive to precise tape head spacing and tape stability. The center seismometer was recorded on a different head from that used on the other seismometers. This should be avoided if a tenth of a second reliability in timing is expected.)

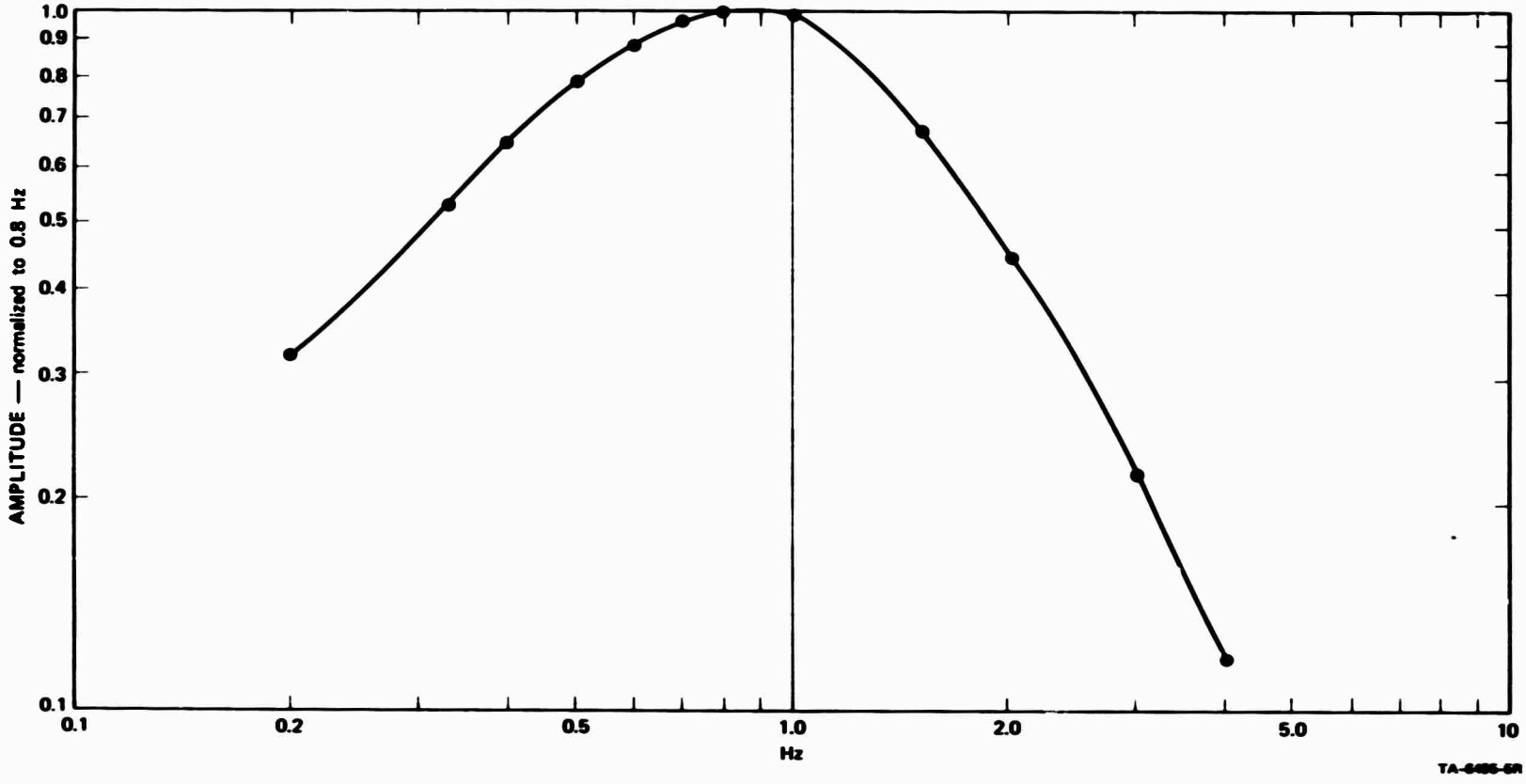

FIGURE 10 SEISMOMETER RESPONSE—TYPICAL CHANNEL

Travel Times

Existing travel-time tables formed a starting point for analysis of BYA observations. Jeffreys and Bullen (J-B), 1940, published tables of predicted PKP travel times based on a two-layered core of the earth. This included predicted times for paths corresponding to the AB, BC, and DEF branches of the travel time curve. As more observational data became available, additional arrivals (precursors) were noted and slight deviations from the J-B tables were seen. In 1968, new tables by Bolt were included in a new set of seismological tables for P phases (Herrin et al., 1968). These included times for a new branch, GH; a consequence of the intermediate core in a tripartite core model. New travel times for the BC branch were not included. These 1968 tables (corrected 2.0 sec for use with J-B P tables) were used in this study.

Appendix A lists good quality PKP arrivals at Byrd used in this analysis. Observed travel times were corrected for the earth's ellipticity according to tables by Jeffreys and Bullen (1967). Depth corrections were taken from Bolt (1968).

Herrin and Taggart (1968) give a station correction for station BYR (USC&GS station located within 100 m of the center BYA seismometer) of 0.24 sec + 0.24 $\sin(Z + 266^{\circ})$, based on 90 observations. Simple calculation of the expected delaying effect of the seismometer's location on 2160 m of ice and at an altitude of 1500 m above sea level yields a station correction of 0.43 sec. An observational check of 82 teleseismic P ($75^{\circ} < \Delta < 95^{\circ}$) arrivals at BYA during 1968 showed an average residual of 0.8 sec (compared to J-B tables). No significant azimuthal dependence was seen.

Due to these discrepancies, no station correction is introduced. Future evaluation of the data may justify further consideration of this factor.

Between about 142 to 152°, relatively high amplitude arrivals are identified. These form a consistant set with sharp onsets (see Fig. 8) but do not fall on any of the branches listed in the 1968 tables. On the basis of the recent literature, these will be referred to as BC arrivals (e.g., Sacks et al., 1970, and Engdahl and Felix, 1970).

These are plotted separately on Figure 11. Each point plotted represents the corrected travel time from a single event. Circles are earthquakes; triangles are suspected blasts (0 km depth by USC&GS). From a total of 115 arrivals, a curve was computed by at least squares fit. The first-order fit:

$$t = 19m\ 31.07726\ sec + 3.00003\ (\Delta - 142^{\circ})\ sec$$

standard error = 0.746 sec

is shown in the figure. Second- and third-order curves were also calculated and are given below:

$$t = 19m\ 30.749\ sec + 3.2447\ (\Delta - 142^{\circ})\ sec - 0.0282003\ (\Delta - 142^{\circ})^{2} sec$$

standard error = 0.726 sec

$$t = 19m\ 30.885\ sec + 2.988\ (\Delta - 142^{\circ})\ sec + 0.04730\ (\Delta - 142^{\circ})^{2} sec - 0.00573871\ (\Delta - 142^{\circ})^{3}\ sec$$

standard error = 0.724 sec

Because of the small difference in standard error, the second- and third-order fits are not justified at this time.

Although some investigators have extended the BC branch to 155° or farther, the sparse BYA data do not confirm extension beyond 152°. The USC&GS shows few earthquakes at these distances; also, the detection threshold appears to be higher for this range. As seen in Figure 8, the BC arrival has, at the least, lost its preeminence.

Arrivals identified as falling on the AB branch were observed at $\Delta > 145^{\circ}$. From $145^{\circ} < \Delta < 152^{\circ}$, however, the AB arrivals follow closely the larger BC signals. From $153^{\circ} < \Delta < 180^{\circ}$, AB arrivals are the largest PKP amplitudes recorded at BYA. Since the detection threshold of AB was lower than that of EF in this range, enough AB arrivals were recorded to confirm the trend and general shape of the published curve. BYA observations, however, were usually later than predicted by several seconds. For instance, the well-recorded events originating at Novaya Zemlya give AB travel times of 1.3 and 1.5 sec greater than predicted. Combined with the EF arrival times previously mentioned, this gives DF-AB intervals of 3.6 to 3.9 sec greater than predicted and show that neither can be adjusted for a different depth of hypocenter without increasing the deviation of the other.

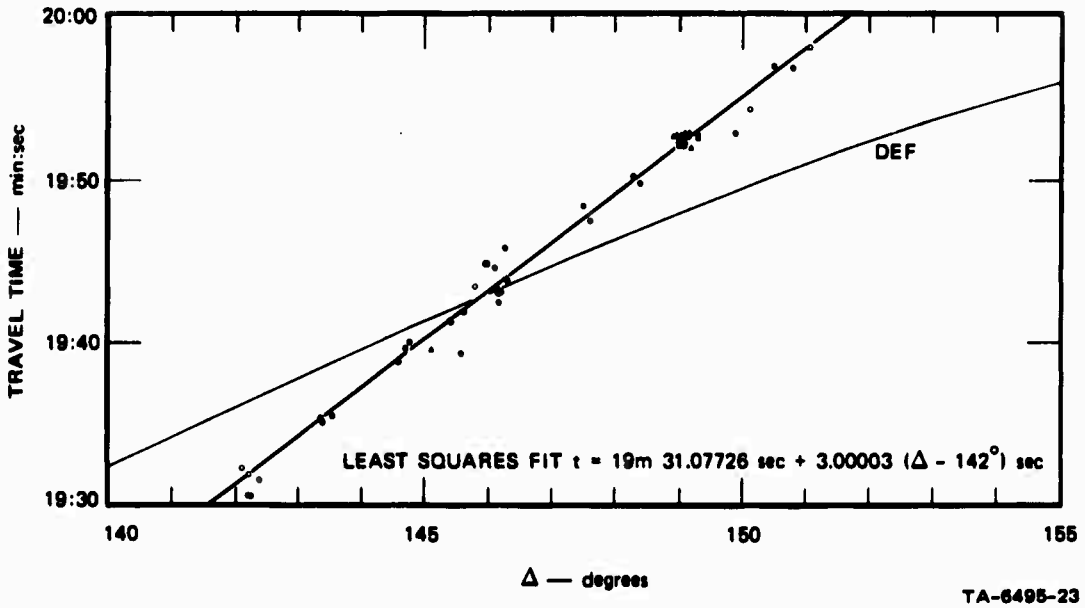

FIGURE 11 BYA TRAVEL TIMES FOR BC BRANCH

Of additional interest on these events at $\Delta = 173^{\circ}$ is seismic energy starting at least 25 sec earlier than the AB arrival (Figure 12). This does not appear to be described in the literature; however, Bolt (personal communication) reports indications of this energy from other events at similar Δ's, and Ergin (1967) shows numerous arrivals between the DF and AB branches.

Source Characteristics

Part of the study of source characteristics has shown that core phases offer some promise in discriminating between earthquakes and explosions. PKP and PKIKP can be used in most of the same ways as teleseismic P. As pointed out by Bolt (1968), they have an advantage in that PKIKP has a sharp onset beyond $\Delta = 160^{\circ}$. PKP has a large amplitude with a sharp onset for $142^{\circ} < \Delta < 152^{\circ}$ on the BC branch. Bolt also notes that the contrast in $dt/d\Delta$ between the AB (denoted by PKP_2) and EF branches for $\Delta > 160^{\circ}$ produces a PKP_2 - PKIKP internal more sensitive to changes in Δ than the S-P interval near $\Delta = 50^{\circ}$. An error of 0.1° in Δ should be detectable.

Examples are shown for earthquakes and Russian nuclear shots of first motion, determination of depth from BC branch travel times, and the sharpness of the PKP_2 - PKIKP interval.

The maximum sensitivity--or lowest detection threshold--appears to fall on the BC branch at $142^{\circ} < \Delta < 152^{\circ}$. Within this range, numerous events of USC&GS magnitude $m_b = 4.5$ and occasionally less are seen even on unenhanced records. Below 142°, there appears a gradual dropping off in amplitude and quality to $\sim 110^{\circ}$. For example:

117°	Nevada Test Site (Boxcar)	$m_b = 6.3$	Yielded 15mμ	Poor onset
147.6°	North-Atlantic earthquake	$m_b = 4.7$	Yielded 40mμ	Good onset

As for P, the first motions of PKP events are possible distinguishing characteristics between explosions and natural earthquakes. Figure 13 shows onsets of arrivals of the BC branch. Trace 1 shows the common case in which explosions show a clearly compressional first motion. However, Trace 2 shows that these are not always clear-cut, especially if only one seismometer trace is examined. (In this case, comparison with traces from

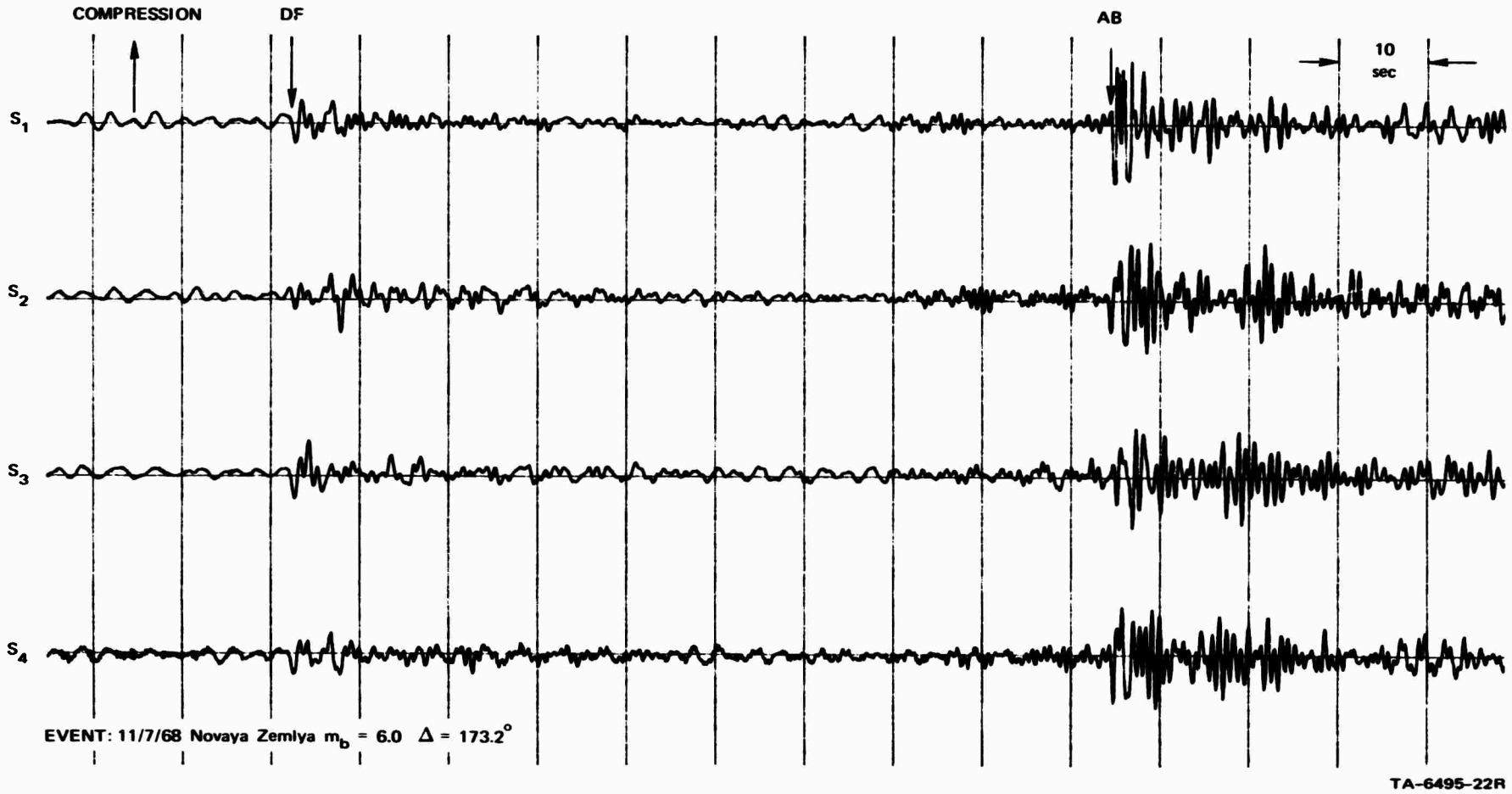

FIGURE 12 DF - AB INTERVAL

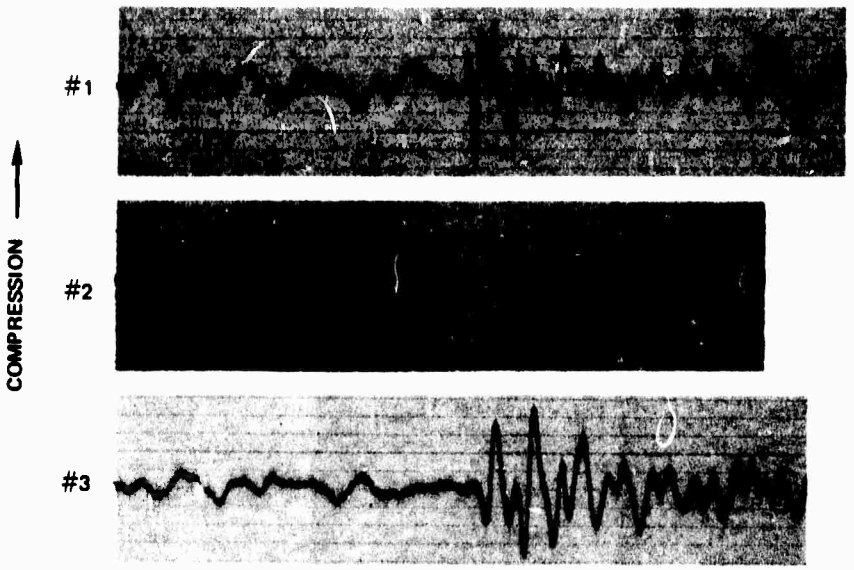

#1	E. KAZAKH BLAST	m_b = 5.4	Δ = 148.9°
#2	E. KAZAKH BLAST	m_b = 5.0	Δ = 149.1°
#3	N. ATLANTIC QUAKE	m_b = 4.7	Δ = 147.6°

TA-6495-19R

FIGURE 13 FIRST MOTIONS

the other recording seismometers shows the true compressional onset.) Although none of the BC arrivals from blasts examined showed clear dilation, such as shown on Trace 3 from a North Atlantic earthquake, onsets from events of $m_b < 5.0$ were unclear from preliminary examinations.

The sharp onsets observed on the BC branch arrivals lead to another distinguishing criterion--depth of hypocenter. Since PKP waves travel along paths nearly normal to the earth's surface, differences in arrival times vary more with hypocenter depth than for other wave paths. For example, if the true onset of a PKP wave could be determined to $\pm$ 0.5 sec and compared with an accurate time prediction of a zero depth event, the hypocenter would be determined to $\pm$ 3 km. (In practice, effects of local geology cannot be completely discounted.) The feasibility of this is examined briefly. The derived curve of Figure 11 was used to predict travel times for surface focus events recorded at Byrd Station. Appendix A shows the results of subtracting these predicted times from the actual travel times without depth correction. The time residual can be used with tables from Bolt (1968) to recalculate hypocenter depth. The depths determined from our residuals are then compared with those depths given by the USC&GS. All those events, presumably explosions, listed at 0 km by the USC&GS also show times corresponding to depths within 5 km of the surface based on the Byrd Station arrival times. The only other event with such a shallow depth determination is an event at Lake Baikal ($\Delta = 151^{\circ}$), which the USC&GS similarly lists as 4 km deep.

The small scatter in BC arrival times allows their use with teleseismic P in least squares solutions for depth determination. The steeper penetration of the crust and upper mantle may make this BC curve more valid as a world average than P travel time. The errors shown by Evernden (1969) in depth determination from average P travel time curves should be less for PKP.

Beyond 152° in Appendix A, there is no immediate attempt to determine hypocenter depth from arrival times because of differences between observed travel time and published values (Bolt, 1968) of several seconds. BYA data were too sparse to justify fitting a curve as done for the BC branch. Arrivals on the DF branch are compared to the Bolt (1968) curve. The greater scatter observed is partly due to interference by precursors.

For $\Delta > 160^{\circ}$, on larger events where DF and AB are both clearly observable, there is another way to determine hypocenter depth that is independent of the USC&GS epicenter solutions. Origin times are still needed. Figure 12 shows the recording of an explosion at Novaya Zemlya, 173° from Byrd. The onset of both DF and AB arrivals are clear on all four seismometers.

At $\Delta \geq 160^{\circ}$, the slope of the AB branch is many times as steep as that of the DF branch. For example, the interval between these branches is increasing at 4.0 sec/deg at 173°. If the AB-DF interval can be picked accurately to 0.4 sec, the Δ is determined to 0.1 deg. Once this confidence can be gained in the true Δ, the depth can be determined by the absolute travel time and predicted travel time curves.

Internal Constitution of the Earth

Checks were made for azimuthal dependence of residuals, both from teleseismic P and PKP arrivals; no dependence was found. In both cases, the majority of USC&GS-listed events occurred in a small range of azimuthal angles. With this limitation, a small variance with azimuth, < 0.4 sec, would not have been detected.

The boundaries of the outer and inner cores are now being determined most accurately by observation of PcP and PKIKP waves. Presently used figures for their mean radii are 3477 km (Taggart and Engdahl, 1968) and 1216 km (Bolt, 1968). GH arrivals, which could confirm the extent and velocity of an intermediate core, are not clearly enough recorded from the small events used in this study for quantitative interpretation. In agreement with Husebye and Toksoz (1969), we find GH arrivals cannot be observed with confidence beyond 145°.

The observed DF-AB interval in $\Delta > 160^{\circ}$ may be caused by deep variation in constitution of the earth. Bolt (personal communication) lacks confidence in his published travel times as a world norm in this range due to systematic anomalies observed in the region of his test data earthquakes (Indian Ocean). Similarly, of course, Byrd Station may exhibit complimentary anomalous features. An alternate hypothesis put forth is that the core of the earth is more spherical than the basic

ellipsoidal figure of the earth. This could retard AB arrivals, yet advance DF ones.

The arrival of energy 25 sec before the AB arrivals at $\Delta = 173^{\circ}$ might be interpreted as a result of an island arc crustal plate dipping into the mantle at Novaya Zemlya. In view of similar observations from different areas, however, we cannot strongly support this conclusion.

Figure 4, shown earlier, plots travel time from well-recorded earthquakes against predicted times. Appendix A lists the events used. Between 125 and 140° there were many more arrivals of good quality, and only the clearest onsets were used. Outside this range, the number of earthquakes were fewer, and consequently all events which appeared reliable appear on the figure. Each segment of the travel time curve will be examined separately.

Arrivals along the DE segment agree closely with predicted times from 110° to just under 140°. Near 140°, there is some interference by earlier arrivals of increasing amplitude (see Figure 8). In Appendix A, these early arrivals are shown without depth calculation. This interference may hide the DE onset or otherwise lead to misinterpretation of later arrivals. BYA results for this range are in full accord with the tables.

Precursors to the DE arrivals were seen on large earthquakes from 110 to 145°. We follow Bolt's nomenclature and call these GH. Although these precursors tend to be emergent in onset, the energy arriving before the DE arrival increases from about 135° up. At $\Delta < 135$, the GH onsets are seldom picked with any confidence. At $\Delta > 142^{\circ}$, there is some question in distinguishing GH arrivals from other energy. Beyond 147°, where time separation would again permit identification of GH, the arrivals seen correspond better with times for BC (again see Figure 8). BYA data can only confirm the existence of precursors to the DF branch and give only mildly supporting evidence for the time of onset of this branch.

At Δ greater than 145°, the EF arrivals were recorded from very few earthquakes. Primarily, there simply were not many earthquakes in this region, but also this branch no longer contains the majority of the energy. From $142^{\circ} < \Delta < 152^{\circ}$, the BC branch dominates, and EF arrivals show up as precursors only on some of the larger ($m_b \geq 5.5$) E. Kazakh events. At $\Delta > 152^{\circ}$, the separation of EF from other arrivals is sufficient

to avoid interference; however, there were not enough large earthquakes for good comparison with published EF values. The clearest records of EF were from two large events at Novaya Zemlya ($\Delta = 173^{o}$). EF arrivals from these were 2.1 and 2.6 sec earlier than predicted (Bolt, 1968).

SUMMARY, CONCLUSIONS, AND RECOMMENDATIONS

A four-element, magnetic-tape-recording, seismograph array was established at Byrd Station, Antarctica. It was run by SRI for the calendar year 1968 and has been operated since by USC&GS personnel.

Byrd Station was found to be a fairly quiet site, seismically, especially within the band of PKP frequencies. Helicorder records were made with system magnification of near 100 K. The limiting factors were the station's "cultural noise" and low frequency background noise, both primarily outside the signal band. The detection threshold for PKP events from unenhanced BYA records is shown in Figure 9. No significant correlation was found between noise levels and local storms. Lack of meteorological data prevented correlation with oceanic storms to the north.

Digital tapes were made of 142 events for examination of data enhancement techniques. Spectral analysis shows the PKP signal energy lies primarily between 0.4 and 2 Hz. Digital filtering passing this band greatly enhances the PKP signals, thereby lowering the detection threshold. Although the BYA array is too small for effective velocity filtering, the straight sum of signals in the array is of some help in observing coherent energy arrivals. The data now on hand could be enhanced even more effectively by computerized optimum filtering. Digitizing the 1969 data would roughly double the data sample to be treated.

Work with records from BYA for the first two years showed that the BC branch of PKP is sharp enough to be promising for depth determination on events with $m_b > 4.8$. A new determination of detection thresholds as a function of Δ can be made after using digital techniques to enhance arrivals on more records. It would be useful to work out an analytical solution for the possible improvement in hypocenter depth determination by adding PKP arrivals to the least squares fit of teleseismic P.

The EF and AB branches offer possibilities in depth determination beyond $\Delta = 160^{\circ}$. Arrays in South Africa, Malagasy, and Kerguelen could be used to monitor western U.S. earthquakes and nuclear shots over a range of Δ to establish any advantages over P depth determination. Arrays should be large enough to determine $dt/d\Delta$ as an aid in separating the various branches near BC.

Operating arrays covering Asia could be established in South America and New Zealand, even if only the BC branch should have a clear advantage over P in depth determination.

Travel times computed from PKP arrivals observed at Byrd show general agreement with recently published tables (Bolt, 1968). Deviation from the most recently published tables include the following: (1) presence of a strong BC branch, (2) lack of confirmation for GH branch at $\Delta > 145^{\circ}$, (3) greater DF-AB interval at $\Delta > 160^{\circ}$, and (4) presence of arrivals between the DF and AB arrivals at $\Delta = 173^{\circ}$.

BIBLIOGRAPHY

Bolt, B. A., 1964, The Velocity of Seismic Waves Near the Earth's Center, Bull. Seism. Soc. Am. Vol. 54, pp. 191-208.

Bolt, B. A., 1968, Estimation of PKP Travel Times, Bull. Seism. Soc. Am., Vol. 58, pp. 1305-1324.

Engdahl, E., 1968, Core Phases and the Earth's Core, Doctor's Thesis, St. Louis University.

Engdahl, E. R., and C. P. Felix, 1970, Array Analysis of Core Phases, Abstract only, Trans. AGU, Vol. 51, pp. 360.

Ergin, Kazim, 1967, Seismic Evidence for a New Layered Structure of the Earth's Core, J. Geophys. Res., Vol. 72, pp. 3669-3687.

Evernden, J. F., 1969, Identification of Earthquakes and Explosions by Use of Teleseismic Data, J. Geophys. Res., Vol. 74, pp. 3828-3856.

Herrin, E. (Chairman)et al., 1968, 1968 Seismological Tables for P Phases, Bull. Seism. Soc. Am., Vol. 58, pp. 1193-1352.

Herrin, E., and J. N. Taggart, 1968, Regional Variations in P Travel Times, Bull. Seism. Soc. Am., Vol. 58, pp. 1325-1338.

Husebye, E., and M. N. Toksoz, 1969, On the Structure of the Earth's Core, in press (referenced in Husebye and Madariaga 1970).

Husebye, E., and R. Madariaga, 1970, The Origin of Precursors to Core Waves, Bull. Seism. Soc. Am., Vol. 60, pp. 939-952.

Isherwood, W. F., 1969, Investigation of PKP Seismic Waves, (prepared for AFOSR under Contract F44620-67-C-0080), Stanford Research Institute, Menlo Park, California, March 1969.

Jeffreys, H., and K. E. Bullen, 1967, Seismological Tables, Gray Milne Trust (First Edition 1940).

Sacks, I. S., G. Soa, and P. Aparicio, 1970, Time Anomalies and Structure Beneath the Andes, Carnegie Institution, Annual Report of the Director, pp. 452-459.

Shahidi, Mohammad, 1968, Variation of Amplitude of PKP Across the Caustic, Phys. Earth Planet. Interior, Vol. 1, pp. 97-102.

Taggart, J. N., and E. R. Engdahl, 1968, Estimation of PcP Travel Times and Depth to the Core, Bull. Seism. Soc. Am., Vol. 58, pp. 1293-1304.

Date	O.T. Hr-Min-Sec	Lat.	Long.	Region	m_b	No. Sta.	Δ°	Compression/ Dilation	T.T. Min-Sec	ϵ_{ij} (sec.)	Period (sec.)	Amp. (mμ)	Digi-tized	Res.for 0 Depth (sec.)	Depth from Res. (km)	C & GS Depth (km)	No. of Seismometers
6/ 6/66	194407.9	14.9N	119.9E	Luzon,PI	5.4	69	109.713	D	18m 24.6	0.7	1.5	4.3	X	6.2	70	80	4
8/28/66	204216.7	15.5N	122.0E	Philippines	5.7	93	110.042	D	18m 10.8	0.7	3.0	24	X			15	4
8/ 3/68	062505.8	18.5N	122.3E	Luzon PI	5.6	101	110.906		17m 58.7	0.8			X			37	4
							110.906		18m 31.8	0.8	2.0	31	X	4.1	26	37	4
11/10/68	170159.2	20.0N	121.4E	Philippines	5.2	80	114.457		18m 38.2	0.8			X	4.7	30	33 N	2
12/16/68	163000.0	37.2N	116.5W	S.Nev.	6.3	159	116.958		18m 46.2	1.3			X	0.8	5		2
6/ 4/66	171509.8	22.5N	121.4E	Taiwan	5.2	56	116.966	C	18m 40.2	0.6	1.0	9.2	X	7.2	48	47	4
2/26/68	105016.7	22.7N	121.5E	Taiwan	6.0	57	117.132	C	18m 31.6	0.6	2.0	18	X			24	3
							117.132	D	18m 43.6	0.6	2.0	63	X	3.9	24	24	3
10/7/68	192020.3	26.3N	140.6E	Bonin Isl.	8.1	67	117.425		17m 47.4	1.0	1.2	580	X	60.8	520	518 D	4
5/ 3/68	053245.7	25.1N	124.6E	NE Taiwan	5.8	67	119.026	D	18m 36.0	1.0	1.1	28	X	12.2	89	98 D	3
11/6/66	170141.1	38.0N	88.5W	S. Illinois	5.3	144	116.077		18m 45.0	1.3			X	8.0	39	16	2
10/18/66	055405.7	24.9N	122.3E	Taiwan	5.1	42	116.148		18m 44.6	1.0	1.2	5.6	X	6.6	43	44	4
10/20/68	070817.1	25.0N	122.5E	Taiwan	5.4	51	119.197		18m 48.6	1.0	2.0	6.8	X	+3.0	18	15	4
2/11/68	121408.6	28.0N	139.5E	Bonin Isl.	4.7	53	119.288	C	17m 51.5	1.1	1.0	25	X	60.1	513	513	3
7/ 8/68	212448.3	28.8N	142.5E	Bonin Isl.	5.3	42	119.566	D	18m 47.3	1.1	2.1	7.9	X	4.9	31	33	4
6/15/68	055859.0	27.0N	126.5E	E.China Sea	5.7	80	120.462	D	18m 41.6	1.0	1.0	2.8	X	12.2	89	88	4
11/12/66	004412.6	27.5N	128.4E	Ryukyu Isl.	5.6	80	120.690		18m 47.5	1.0			X	6.6	46	48 D	2
5/ 4/66	032126.3	29.7N	138.0E	S.Honshu,Jap.	4.4	31	121.238	C	17m 57.4	1.1	0.6	8.0	X	56.0	492	484	3
7/22/66	223343.2	30.3N	138.4E	S.Honshu,Jap.	5.0	48	121.753	D	18m 03.8	1.1	1.0	16	X	52.5	440	438 D	4
10/29/66	040604.1	31.2N	141.6E	S.Honshu,Jap.	5.7	76	122.036		18m 54.8	1.2	1.5	7.6	X	2.0	13	17	4
10/16/68	074546.8	26.3N	129.4E	Ryukyu Isl.	5.6	75	122.253		18m 55.5	1.1	2.0	7.6	X	1.8	12	13	4
5/14/68	140506.0	29.9N	129.4E	Ryukyu Isl.	5.6	102	122.614	D	18m 37.2	1.1	1.4	180	X	21.3	174	168 D	4
5/8/66	121713.4	43.6N	127.9W	W. of Ore.	6.1	46	123.366	D	18m 56.1	1.5	0.9	2.6	X	2.9	18	33	3
6/ 6/68	192247.8	31.0N	131.9E	Kyushu,Jap.	5.7	93	123.514	D	18m 55.1	1.1	1.0	130	X	4.6	29	36	4
9/15/68	145229.4	33.1N	142.0E	E. of Honshu	4.7	31	123.781	C	18m 53.3	1.2	1.0	1.2	X	6.8	45	53	4
10/28/68	144041.4	33.4N	140.8E	S.of Honshu	5.5	70	124.343		18m 53.5	1.2	1.2	10	X	7.8	53	61	4
2/28/68	120801.5	32.9N	137.7E	S.of Honshu	5.8	88	124.382		17m 54.4	1.2			X			349	3
							124.382	C	18m 16.1	1.2	1.0	180	X	42.2	345	349	3
4/ 1/68	071317.8	32.3N	132.1E	Shikoku,Jap.	5.7	98	124.765	D	18m 57.6	1.2	2.4	37	X	4.4	28	32	3
4/1/68	004204.2	32.5N	132.2E	Shikoku,Jap.	6.1	133	124.943	C	18m 57.6	1.2	2.2	280	X	4.5	29	33	3
12/11/68	114530.8	33.6N	134.0E	Shikoku,Jap.	5.4	58	125.668		18m 58.7	1.2			X	5.1	33	32 D	2
6/ 5/66	161704.6	33.3N	132.2E	Shikoku,Jap.	6.3	56	125.717	C	18m 58.0	1.2	2.0	230	X	5.9	38	41	4
6/ 6/68	042103.2	33.4N	132.2E	Shikoku,Jap.	5.1	40	125.871	C	18m 58.2	1.2	2.0	10	X	6.0	39	43 D	4
10/8/66	005041.8	35.6N	136.9E	S.of Honshu	5.3	56	126.598		18m 55.2	1.3	1.2	3.4	X	10.3	74	78	4
7/ 1/66	104511.6	36.0N	136.3E	Honshu, Jap.	5.6	85	127.116	C	18m 57.8	1.3	1.8	120	X	8.7	81	87	4
8/ 8/68	045510.0	36.4N	141.4E	E.of Honshu	5.4	55	127.137	D	18m 00.6	1.3	1.6	10	X	5.7	37	41 D	4
8/ 2/68	133023.3	27.5N	60.8E	S.Iran	5.7	50	127.432	D	18m 56.6	1.0	1.5	33	X	6.3	57	62 D	4
6/14/68	134831.2	28.4N	53.1E	S.Iran	5.6	104	128.261	C	19m 04.6	1.1	2.0	25	X	4.3	27	33 N	4

Date	O.T. Hr-Min-Sec	Lat.	Long.	Region	m_b	No. Sta.	Δ°	Compression/ Dilation	T.T. Min-Sec	ϵ_{ij} (Sec.)	Period (Sec.)	Amp. (mμ)	Digi-tized	Res.for 0 Depth (Sec.)	Depth From Res. (km)	C & GS Depth (km)	No. of Seismometers

Date	D.T. Hr-Min-Sec	Lat.	Long.	Region	m_b	No. Sta.	Δ°	Compression/ Dilation	T.T. Min-Sec	ϵ_{ij} (sec)	Period (sec)	Amp. (mμ)	Digi-tized	Res. for 0 Depth (sec)	Depth from Res. (km)	C & GS Depth (km)	No. of Seismometers
2/25/68	200031.5	37.6N	141.4E	E.of Honshu	5.5	76	128.315	D	19m 59.8	1.3	1.9	20	X	9.0	63	66	3
9/ 3/68	070136.5	37.9N	141.7E	E.of Honshu	5.4	54	128.598	C	19m 59.2	1.3	1.5	16	X	9.6	68	79 D	4
7/ 5/68	112812.6	38.5N	142.0E	E.of Honshu	5.9	121	129.080	C	19m 04.1	1.3	2.2	130	X	6.2	40	43	4
6/12/68	175201.2	39.1N	142.9E	E.of Honshu	5.5	74	129.554	C	19m 07.4	1.3	2.0	23	X	3.7	23	30 R	4
6/12/68	215741.3	39.3N	142.8E	E.of Honshu	5.7	90	129.718	D	19m 06.3	1.3	1.4	28	X	5.2	33	36 D	4
6/15/68	033118.3	39.3N	142.8E	E.of Honshu	5.4	54	129.736	D	19m 06.8	1.3	2.0	16	X	2.6	16	25	4
6/13/68	211035.4	39.4N	142.9E	E.of Honshu	5.5	70	129.785	D	19m 07.8	1.3	1.4	28	X	3.8	24	29	4
7/12/88	004436.5	39.5N	143.2E	E.of Honshu	6.0	78	129.860	D	19m 06.3	1.3	2.0	110	X	3.4	21	28	4
6/18/68	013817.4	38.5N	142.9E	E.of Honshu	5.3	59	129.869	C	19m 07.2	1.3	2.0	14	X	4.6	29	33	3
7/12/68	035627.5	39.5N	143.2E	E.of Honshu	5.5	64	129.877	C	19m 09.7	1.3	2.0	54	X	2.1	13	26	4
6/12/88	134150.7	39.5N	142.7E	E.of Honshu	6.0	102	129.915	C	19m 05.6	1.3	2.0	450	X	4.3	27	44 D	4
5/20/88	031619.6	40.0N	144.0E	E.of Honshu	5.5	40	130.165	C	19m 09.5	1.4	1.5	4.0	X	2.7	18	31 D	4
5/18/68	230454.7	38.9N	143.1E	E.of Honshu	5.8	101	130.191	C	19m 07.3	1.4	1.2	10	X	5.0	32	37	4
11/13/88	184147.8	40.2N	147.5E	E.of Honshu	5.5	59	130.572		19m 07.0	1.4			X	8.0	39	49	2
7/ 9/68	062823.0	40.4N	143.7E	E.of Honshu	4.8	37	130.654	C	19m 09.1	1.4	1.9	11	X	4.0	25	33	3
11/24/68	212059.9	40.3N	142.3E	E.of Honshu	5.9	133	130.702		19m 06.3	1.4			X	8.9	46	51 D	2
5/16/68	004855.4	40.8N	143.2E	E.of Honshu	5.9	115	131.147	D	19m 15.1	1.4	2.0	63	X	-1.0	- 6	7	4
9/15/68	105011.8	40.8N	143.2E	E.of Honshu	5.4	93	131.206	D	19m 12.5	1.4	1.2	15	X	1.7	10	15	4
5/16/68	184321.0	40.7N	142.1E	E.of Honshu	5.7	102	131.215	D	19m 06.9	1.4	2.6	42	X	7.3	49	59	4
5/24/68	140624.2	40.8N	143.0E	E.of Honshu	5.6	55	131.272	C	19m 10.6	1.4	1.5	5.3	X	3.7	23	38	4
6/17/68	115300.4	41.0N	143.0E	Hokkaido,J.	5.7	95	131.323	C	19m 10.5	1.4	2.2	64	X	3.8	24	48 D	4
5/16/68	063651.0	41.1N	143.0E	Hokkaido,J.	5.7	77	131.425	D	19m 10.8	1.4	0.9	10	X	3.8	23	35	4
5/16/68	191647.2	41.3N	142.4E	Hokkaido,J.	5.6	75	131.744	C	19m 11.1	1.4	1.5	20	X	4.1	26	42 D	4
5/16/68	202214.9	41.4E	142.6E	Hokkaido,J.	5.6	74	131.805	C	19m 12.2	1.4	2.0	28	X	3.1	19	39 D	4
5/16/68	103901.6	41.5E	142.7E	Hokkaido,J.	6.3	136	131.859	C	19m 12.9	1.4	2.0	950	X	2.5	15	33	4
5/22/68	105153.3	41.5E	142.8E	Hokkaido,J.	5.9	83	131.877	C	19m 10.1	1.4	2.0	32	X	5.4	35	40 D	4
							131.877		19m 11.3	1.4			X	4.2	28	40	4
10/7/68	204901.3	42.0N	142.4E	Hokkaido,J.	5.7	101	132.426		19m 12.4	1.4	2.4	58	X	4.1	26	32	4
9/21/68	130558.2	42.2N	142.6E	Hokkaido,J.	5.9	167	132.522		19m 56.5	1.4	2.0	3.6	X			33	3
							132.547		19m 12.4	1.4	2.0	140	X	4.3	27	33	4
2/ 3/68	113044.4	43.2N	146.8E	Kurile Is.	5.0	30	132.776	D	19m 13.6	1.5	1.0	12	X	3.5	22	46	2
7/22/68	001353.0	42.3N	142.3E	Hokkaido,J.	4.7	45	132.901	D	19m 14.2	1.5	1.1	7.4	X	3.1	19	31 D	4
8/ 7/68	080013.4	43.1N	144.6E	Hokkaido,J.	5.6	64	133.080	C	19m 11.3	1.5	1.0	5.6	X	6.4	42	54 D	4
1/29/68	101905.6	43.6N	146.7E	Kurile Is.	6.3	168	133.220	D	19m 12.5	1.5	2.0	270	X	5.4	35	40	3
7/27/68	024549.2	35.4N	27.8E	Dodecanese I.	5.0	54	133.515	D	19m 16.6	1.3	1.0	1.7	X	2.1	13	20	4

Date	O.T. Hr-Min-Sec	Lat.	Long.	Region	m_b	No. Sta.	Δ°	Compression/ Dilation	T.T. Min-Sec	ϵ_{ij} (Sec.)	Period (Sec.)	Amp. (mμ)	Digi-tized	Res.for 0 Depth (Sec.)	Depth From Res. (km)	C & GS Depth (km)	No. of Seismometers

Date	O.T. Hr-Min-Sec	Lat.	Long.	Region	m_b	No. Sts.	Δ°	Compression/ Dilation	T.T. Min-Sec	ϵ_{ij} (sec.)	Period (sec.)	Amp. (mμ)	Digi-tized	Ses. for 0 Depth (sec.)	Depth from Ses. (km)	C & GS Depth (km)	No. of Seismometers
5/30/99	174024.4	35.5N	28.0E	E.Med.Sea	5.3	97	133.577	C	19m 15.7	1.3	1.0	40	X	3.1	19	20	4
5/30/98	052348.9	44.7N	150.3E	Sarile Isl.	5.5	101	133.837	C	19m 12.5	1.6	1.0	2.9	X	8.1	39	48 D	4
5/20/98	210944.8	44.8N	150.3E	Surile Isl.	5.8	44	133.804	C	19m 13.3	1.8	1.1	36	X	5.9	36	38	4
9/4/98	232447.2	34.0N	58.2E	Iran	5.4	95	133.877	C	19m 17.3	1.3	1.5	17	X	2.1	13	15	4
5/21/98	082000.9	44.8N	150.2E	Karile Isl.	5.7	88	133.887		19m 12.9	1.9	2.2	56	X	6.3	41	33	4
9/ 1/69	072730.2	34.0N	59.2E	Iran	5.9	91	133.947	0	19m 13.5	1.3	1.2	4.2	X			15	3
							133.947		19m 19.8	1.3			X			15	
12/5/98	075211.0	36.9N	27.0E	Dodecanese	5.5	80	134.573		19m 11.1	1.3			X			35	2
10/31/89	032215.0	36.9N	27.1E	Dodecanese	5.1	46	134.581		19m 19.9	1.3	1.0	10	X	1.8	11	11	4
2/ 3/99	032818.9	46.9N	152.6E	Karile Isl.	5.3	79	135.054	0	19m 19.3	1.8	0.7	17	X	5.0	32	45	1
1/19/88	070204.4	45.0N	143.2E	Hokkaido,J.	9.4	140	135.150		19m 40.5	1.8			X			204	2
							135.150		19m 43.7	1.8			X			204	2
7/25/68	105031.5	45.7N	146.7E	Kurile Isl.	5.8	85	135.294		19m 18.4	1.8	1.5	76	X	2.4	14	17	4
7/ 4/98	214755.8	37.8N	23.2E	S.Greece	5.3	90	135.367	C	19m 19.5	1.3	1.0	5.4	X	5.7	37	33	4
12/19/88	051751.7	36.1N	70.1E	Qimda Kash	5.4	34	135.855		19m 05.4	1.3			X	17.7	143	151	2
12/15/88	021417.5	51.6N	175.8E	Sat Isl.	5.7	82	136.290		19m 17.3	1.8			X	6.2	40	33 N	2
5/20/98	103416.9	48.8N	154.7E	Kurile Isl.	5.4	47	136.995	0	19m 09.8	1.7	0.8	1.3	X			40	3
							136.895	C	19m 19.8	1.7	1.0	30	X	8.1	39	40	4
1/ 3/99	031839.1	37.1N	57.9E	Iran	5.6	47	136.975		19m 24.5	1.3			X	0.8	5	11	2
2/19/98	224541.2	39.4N	25.0E	Aegean Sea	5.9	109	137.109	0	19m 21.3	1.3	1.0	30	X			7	3
2/ 3/89	085706.8	49.4N	155.9E	Kurile Isl.	5.4	50	137.273		19m 11.1	1.7			X			33 N	2
10/24/99	223550.9	49.7N	155.8E	Kurile Isl.	5.5	52	137.530		19m 11.3	1.7	1.0	4.0	X			35	4
8/24/89	041954.5	39.2N	40.2E	Turkey	5.1	42	138.366	0	19m 27.8	1.3	1.1	3.2	X	0.3	2	14	4
12/30/98	070311.7	57.6N	151.4W	Sodisk Isl.	5.4	104	138.514		19m 12.9	2.0			X			34	2
							138 514		19m 23.5	2.0			X	4.0	25	34	2
5/21/89	035911.5	38.9N	65.2E	SK Uzbek SSR	5.4	91	138.760	C	19m 27.3	1.3	1.0	2.6	X	1.3	8	13	4
7/21/98	210231.5	49.7N	147.8E	Okhotsk Sea	4.9	64	138.878		19m 13.2	1.7	0.8	8.8	X			576 0	4
							138.878		19m 22.7	1.7			X			578 0	4
6/15/98	112732.8	51.7N	159.4E	E.Kamchatka	5.4	80	138.914	C	19m 13.4	1.8	0.9	7.8	X			39 0	4
2/19/98	142342.8	49.7N	147.7E	Okhotsk Sea	4.7	94	138.949	C	19m 11.2	1.7	1.9	19	X			582	3
4/23/98	202914.5	58.7N	150.0W	Alaska Gulf	9.3	58	139.526	C	19m 19.5	2.0	2.0	82	X			23	3
5/24/99	213711.2	54.2N	169.3E	Komandorsky	4.7	62	139.742		19m 25.9	1.9	1.0	2.8	X			5	4
9/ 3/98	081952.2	41.6N	32.3E	Turkey	5.7	57	140.251	0	19m 22.7	1.4	1.5	7.3	X			5	3
							140.251	D	19m 36.3	1.4	1.8	34	X			5	4
2/29/98	154619.2	52.8N	157.5E	Kamchatka	5.4	88	140.274		19m 03.5	1.8	0.8	2.9	X			151	3
9/ 4/99	103429.4	53.2N	159.7E	E. Kamchatka	4.7	34	140.300		19m 17.5	1.9			X			31	4
							140.300	C	19m 27.3	1.9	1.0	1.0	X			31	4
1/20/99	142011.5	54.9N	166.0E	Komandorsky	9.1	134	140.905		19m 21.5	1.9			X			23	2
12/17/88	120215.0	60.2N	152.8W	S.Alaska	5.9	101	141.177		19m 13.7	2.1			X			86	2
7/28/99	211239.1	55.4N	166.6E	Komandorsky	5.4	81	141.363	0	19m 24.1	1.8	1.7	52	X			27	4

Date	O.T. Hr-Min-Sec	Lat.	Long.	Region	m_b	No. Sts.	Δ°	Compression/ Dilation	T.T. Min-Sec	ϵ_{ij} (sec.)	Period (sec.)	Amp. (mμ)	Digi-tized	Ses. for 0 Depth (sec.)	Depth from Ses. (km)	C & GS Depth (km)	No. of Seismometers

Date	O.T. Hr-Min-Sec	Lat.	Long.	Region	a_b	No. Sta.	Δ°	Compression/ Dilation	T.T. Min-Sec	t_{ij} (Sec.)	Period (Sec.)	Amp. ($m\mu$)	Digi-tized	Res.for 0 Depth (Sec.)	Depth From Res. (km)	C & GS Depth (km)	No. of Seismometers
3/14/69	020836.6	42.3N	66.5E	C. Kazakh	5.4	17	142.112	C	19m 25.6	1.5	1.7	8.9	E	4.2	28	33	3
3/13/68	223838.9	42.4N	66.5E	C. Kazakh	5.2	19	142.212	C	19m 25.4	1.5	1.0	2.6	E	4.9	32	33	3
9/14/69	011345.2	55.6N	162.1E	E. Kamchatka	5.3	53	142.216	C	19m 19.1	1.9	1.0	2.5	X	10.8	80	70	4
1/26/69	150532.7	55.8N	162.9E	E. Kamchatka	5.5	74	142.256		19m 26.2	1.9				3.9	25	16	2
1/22/69	004230.0	55.9N	163.0E	E. Kamchatka	5.5	87	142.371		19m 24.6	2.0			X	5.7	36	33	2
5/ 1/99	040008.7	44.0N	77.9E	E. Kazakh	4.9	25	143.350		19m 26.2	1.5				7.5	53	53	1
2/ 9/66	132253.9	45.6N	26.4E	Rumania	4.6	9	143.388	D	19m 17.6	1.6	0.9	3.0		15.9	124	122	3
10/20/69	231504.0	45.7N	26.6E	Rumania	4.6	52	143.535		19m 19.1	1.6	0.9	2.4	E	19.0	125	123	4
7/17/69	205504.3	64.0N	147.3W	C. Alaska	4.5	17	144.635		19m 33.5	2.2				3.3	21	20	1
11/16/69	195740.3	64.1N	147.5W	C. Alaska	4.4	28	144.747		19m 32.6	2.2				4.4	29	30	1
7/17/69	205137.5	64.1N	147.9W	C. Alaska	4.9	35	144.753		19m 33.1	2.2				4.1	27	31	1
9/26/99	065955.9	45.9N	42.5E	S.W. Russia	5.6	62	145.143		19m 38.2	1.6				.9	5	0	1
9/ 8/68	162258.6	64.8N	147.6W	C. Alaska	4.5	24	145.420		19m 37.0	2.2	1.0	3.4	X	2.2	14	12	4
9/ 5/69	085745.3	46.7N	82.2E	Kazakh-Sinklang	4.7	14	145.691		19m 35.3	1.6	0.9	1.9	X	5.3	35	33	4
7/31/99	120644.5	64.9N	151.2W	C. Alaska	4.4	32	145.789		19m 32.1	2.2				8.2	58	33	1
9/13/69	215426.5	57.9N	32.4E	9. Atlantic	4.5	19	145.629		19m 36.4	2.0	0.8	1.1		4.2	29	33	4
9/20/69	005651.3	58.1N	32.2W	6. Atlantic	5.0	39	145.987		19m 37.9	2.0				3.1	20	33	1
9/20/99	011304.9	58.1N	32.1E	6. Atlantic	5.2	25	146.004		19m 37.9	2.0				3.3	21	33	1
9/20/69	010738.4	58.2N	32.1E	6. Atlantic	5.0	46	146.099		19m 37.6	2.0				3.8	25	33	1
9/20/99	032429.8*	59.3N	32.3W	N. Atlantic	4.4	8	146.191		19m 36.3	2.0				5.3	35	33	1
11/13/69	120339.9	58.3N	32.7W	6. Atlantic	4.6	24	146.165		19m 35.5	2.0			X	6.1	41	33	2
9/20/69	050857.6	58.3N	32.2W	N. Atlantic	5.6	72	146.176		19m 36.0	2.0				5.7	38	33	1
10/29/96	221915.6	65.4N	150.1W	Alaska	9.0	105	146.209		19m 39.9	2.2	2.0	360.0	X	1.7	11	7	4
9/19/69	205412.4*	59.4N	32.3W	N. Atlantic	4.5	12	146.256		19m 38.9	2.0				3.2	20	33	1
9/19/69	232159.1*	58.4N	32.3E	9. Atlantic	4.6	10	146.256		19m 36.9	2.0				5.1	34	33	1
9/20/99	002050.4*	59.4N	32.1E	6. Atlantic	4.4	10	146.290		19m 36.6	2.0				5.2	34	33	1
7/ 1/99	040201.7	47.9N	48.0E	W. Kazakh	5.5	62	147.495	C	19m 41.7	1.7	1.0	41.0	X	4.2	29	33	4
7/ 3/69	095527.0*	59.4N	30.4E	N. Atlantic	4.7	14	147.607	D	19m 40.4	2.1	2.0	40.0	X	5.5	37	33	4
10/28/69	004600.5*	68.2N	136.5W	9. Yukon	4.2	6	146.278		19m 43.0	2.2				4.9	32	33	1
4/ 6/69	192239.4	50.3N	91.2E	USSR-Mongolia	4.6	26	146.410		19m 43.3	1.6				5.3	35	31	3
7/12/69	120757.2	49.7N	76.1E	E. Kazakh	5.4	51	146.949	C	19m 47.1	1.7	0.6	16.0	X			0	4
									51.0	1.7			X	-.7	-4	0	4
12/18/69	050157.0	49.7N	78.1E	E. Kazakh	5.2	55	146.984	C	19m 51.0	1.7				-.7	-4	0	2
7/ 4/69	024657.0	49.7N	76.2E	E. Kazakh	5.3	70	149.006	C	19m 50.4	1.7				0	0	0	1
9/11/69	040157.1	49.7N	78.1E	E. Kazakh	5.0	28	149.013	C	19m 50.9	1.7				-.5	-3	0	1
9/ 5/68	040557.4	49.8N	78.1E	E. Kazakh	5.5	68	149.034	D	19m 46.0	1.7	0.6	1.0	X			0	4
								C	50.5	1.7	0.9	40.0		-.1	-1	0	4
9/29/96	034257.5	49.8N	79.2E	E. Kazakh	5.6	90	149.043		19m 46.5	1.7	1.5	9.3	E			0	4
									50.7	1.7	0.9	110.0	X	-.3	-2	0	4

Date	O.T. Hr-Min-Sec	Lat.	Long.	Region	a_b	No. Sta.	Δ°	Compression/ Dilation	T.T. Min-Sec	t_{ij} (Sec.)	Period (Sec.)	Amp. ($m\mu$)	Digi-tized	Res.for 0 Depth (Sec.)	Depth From Res. (km)	C & GS Depth (km)	No. of Seismometers

Date	O.T Hr-Min-Sec	Lat.	Long.	Region	m_b	No. Sta.	Δ^o	Compression/ Dilation	T.T. Min-Sec	ϵ_{ij} (Sec.)	Period (Sec.)	Amp. (mμ)	Digi-tized	Res.for 0 Depth (Sec.)	Depth From Sea. (km)	C & GS Depth (km)	No. of Seismometers
11/ 9/88	025357.7	49.8N	76.0E	E. Kazakh	4.9	28	149.065		19m 51.1	1.7				-.6	-4	0	2
4/24/66	103557.1	49.8N	76.1E	E. Kazakh	5.0	34	149.079	C	19m 51.1	1.7	1.0	15.0	X	-.5	-3	0	3
3/ 7/69	082857.5	49.8N	76.2E	E. Kazakh	5.5	67	149.079	C	19m 46.4	1.7						0	4
									50.6	1.7				-.2	-1	0	4
10/ 1/69	040257.6	49.8N	76.2E	E. Kazakh	5.3	59	149.106	C	19m 50.4	1.7				+.2	+1	0	1
5/16/89	040257.1	49.9N	78.1E	E. Kazakh	5.3	83	149.112	C	19m 50.6	1.7				0	0	0	1
6/11/69	030557.6	49.8N	78.2E	E. Kazakh	5.3	53	149.115		19m 50.6	1.7	1.0	10.0	X	0	0	0	4
6/19/68	050557.3	50.0N	79.1E	E. Kazakh	5.5	45	149.170		19m 46.6	1.7	1.0	2.6	X			0	4
									51.2	1.7	1.0	49.0	X	-.4	-2	0	4
7/23/69	024658.1	49.9N	76.3E	E. Kazakh	5.5	56	149.199	C	19m 50.3	1.7				.6	+4	0	1
6/20/68	040558.1	50.0N	78.0E	E. Kazakh	4.8	22	149.316		19m 50.9	1.7	0.6	3.0		.4	2	0	1
5/31/69	050156.6	50.0N	77.7E	E. Kazakh	5.4	50	149.337	C	19m 51.1	1.7				.4	2	0	1
10/30/69	121722.3	52.3N	95.8E	C. Russia	4.8	35	149.897		19m 46.1	1.8				6.9	48	33	4
7/21/68	014119.5	55.2N	113.3E	E. Baikal	5.1	35	150.158		19m 47.5	1.9	2.1	27.0	X	6.2	42	33	4
4/21/89	171834.2	61.9N	26.7W	Iceland	4.6	24	150.501		19m 49.6	2.2				4.6	30	33	1
8/31/68	180635.7	56.3N	115.6E	E. Baikal	4.6	19	150.791		19m 51.1	2.0	1.8	10.0	X	4.3	28	25	4
11/26/68	183151.8	55.9N	111.4E	L. Baikal	5.1	56	151.094		19m 55.6	2.0			X	.7	4	4	2
12/ 5/68	094411.0	83.9N	21.7W	Iceland	5.5	99	153.340		19m 53.4	2.2			X			5	2
									20m 13.8	2.2			X			5	2
9 9 68	022057.9	66.1N	142.1E	E.Siberia	5.1	47	155.400	U	19m 57.0	2.2	1.2	4.0	X			33	4
									20m 03.0								
									20m 16.3								
5 5 69	214731.7	66.8N	18.2W	Iceland	5.2	52	156.470		20m 22.3	2 2						33	1
9 2 69	045957.4	57 4N	54.9E	W. Russia	4 9	34	157.215		20m 27.3	2.0						0	2
9 8 69	045956.1	57.4N	55.1E	Ural Mts	4 9	27	157 220		20m 28.2	2.0						0	4
3 7 68	072742 7	71.8N	3.5W	Jan Mayen	4.9	28	163 299	0	20m 50.9	2.3	2.0	4.0				33	3
4 7 69	202629.9	76 5N	130.8E	Laptev Sea	5.5	82	166 113		19m 59.0	2.4						33	4
									21m 2.9	2.4						33	4
8 22 69	194056 1	76.9N	130.8E	Laptev Sea	4.8	20	166.471		21m 5.9	2 4						33	1
4 21 69	222759 5	74.2N	9.7E	Greenland Sea	5.0	52	167.713		21m 18.0	2.4						33	4
4 19 69	022655.4	74 4N	10.1E	Norwegian Sea	4 5	14	167.860		21m 9.6	2 4						33	1
12 30 68	102709.7	76.2N	7.5E	Svalbard	5 0	44	168.858		20m 9.3	2.4			X			23	2
									21m 17.3	2 4			X			23	2
4 7 68	051624.9	81.5N	3.9W	N.Svalbard	5.3	53	169.995	C	21m 20.2	2.5	0.8	1.3	X			33	3
10 14 69	070008.2	73 4N	54.8E	Novaya	6 1	127	173.214		20m 6.8	2.4						0	1
				Zemlya			173.229		21m 38.8	2.4						0	4
11 7 68	100205.3	73.4N	54.9E	Novaya	6 0	134	173.237		20m 7.3	2.4	1.0	22.0	X			0	4
				Zemlya					21m 39.0	2.4	1.0	39.0	X			0	4

Date	O.T Hr-Min-Sec	Lat.	Long.	Region	m_b	No. Stn.	Δ^o	Compression/ Dilation	T.T. Min-Sec	ϵ_{ij} (Sec.)	Period (Sec.)	Amp. (mμ)	Digi-tized	Res.for 0 Depth (Sec.)	Depth From Sea. (km)	C & GS Depth (km)	No. of Seismometers

NOTES FOR APPENDIX A

O. T. — origin time as calculated by USC&GS

* — Epicenter determination considered by USC&GS as less accurate than others.

Lat., Long. as calculated by USC&GS.

m_b — body wave magnitude as calculated bu USC&GS.

No. Sta. — number of stations used in C&GS computation.

Δ^o — geocentric angle between seismometers and epicenter- average used when pick taken from more than one seismometer.

Compression/dilation - first motion where noted.

T.T. — absolute travel time. When two travel times are listed, the first is DF and the second is either BC or AB.

ϵ_{ij} — ellipticity correction- from Jeffreys and Bullen 1967.

Period — visual appraisement.

Amp. — peak amplitude based on instrument calibration (two place accuracy only).

Digitized — X indicates digital records were made (by Vela Digitizing Center, Alexandria, Virginia).

Residual for 0 depth

Predicted time minus travel time where predicted time is based on first order least squares fit for the BC arrivals (depth corrected using A. Qamar's tables (Bolt, 1968) for Point B and travel times have been corrected for the earths ellipticity.

Depth from Res.

Using A. Qamar's tables (Bolt, 1968) for Point B C&GS depth - 33 km is used where C&GS considers "N" or normal depth.

No. of seismometers

the number of seismometers from which the BYA picks were made and averages taken. The 1970 records are generally only from 1; the helicorder record. Others, 2, 3, and 4 are functions of playback equipment used.


BYRD LAND
ANTARCTICA
SRI
SEISMIC STATION

UNCLASSIFIED

Security Classification

DOCUMENT CONTROL DATA - R & D

(Security classification of title, body of abstract and indexing annotation must be entered when the overall report is classified)

1. ORIGINATING ACTIVITY *(Corporate author)*

STANFORD RESEARCH INSTITUTE

2a. REPORT SECURITY CLASSIFICATION

UNCLASSIFIED

2b. GROUP

NA

3. REPORT TITLE

INVESTIGATION OF PKP SEISMIC WAVES

4. DESCRIPTIVE NOTES *(Type of report and inclusive dates)*

Scientific..... Final

5. AUTHOR(S) *(First name, middle initial, last name)*

William F. Isherwood

6. REPORT DATE	7a. TOTAL NO. OF PAGES	7b. NO. OF REFS
September 1970	40	15

8a. CONTRACT OR GRANT NO.	9a. ORIGINATOR'S REPORT NUMBER(S)
F44620-67-C-0080	6495
b. PROJECT NO. 8652	
c. 62701D	9b. OTHER REPORT NO(S) *(Any other numbers that may be assigned this report)* AFOSR 70-2269TR
d.	

10. DISTRIBUTION STATEMENT

1. This document has been approved for public release and sale; its distribution is unlimited.

11. SUPPLEMENTARY NOTES	12. SPONSORING MILITARY ACTIVITY
TECH, OTHER	Air Force Office of Scientific Research 1400 Wilson Boulevard (SRPG) Arlington, Va. 22209

13. ABSTRACT

A four-element seismic array was established at Byrd Station, Antarctica, for investigation of PKP seismic waves. This seismic station (BYA) has been operating continuously since January 18, 1968. Seismic data are recorded on magnetic tape at a level permitting playback at a system magnification of as high as 500,000. Background ground motion amplitudes at Byrd Station were found to be in the order of 10 millimicrons at the outlying seismometers and frequently of the order of 100 millimicrons at the center seismometer when heavy equipment was operating, nearby. About 2,700 compressional and shear arrivals were reported in the first 8 months of recording, with epicenters ranging over the entire earth. About 400 of these events have been confirmed as PKP arrivals. The epicentral distance for these arrivals ranged from 110° to 173°, with the majority being from the Japanese and Kurile areas. Data from the first full year of operation are now being processed at SRI. The station was turned over to the USC&GS and is currently being operated by that agency.

Key Words:

Seismology
Wave Propagation
Earth's Core
Core Phases
PKP
p'
Antarctica Operation Deep Freeze 1968

DD FORM 1 NOV 65 1473 (PAGE 1)

UNCLASSIFIED

Security Classification